UT-SNU Exchange Lecture Courses (2009 Winter/Autumn)

Bio-inspired Materials and System Design

Novel cell culture system

3.

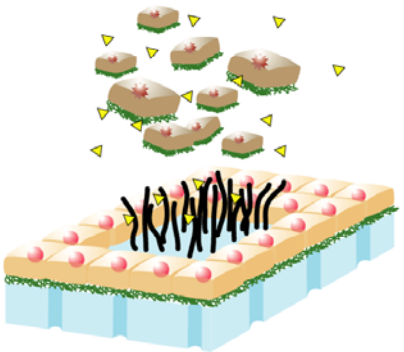

Biofuel cell

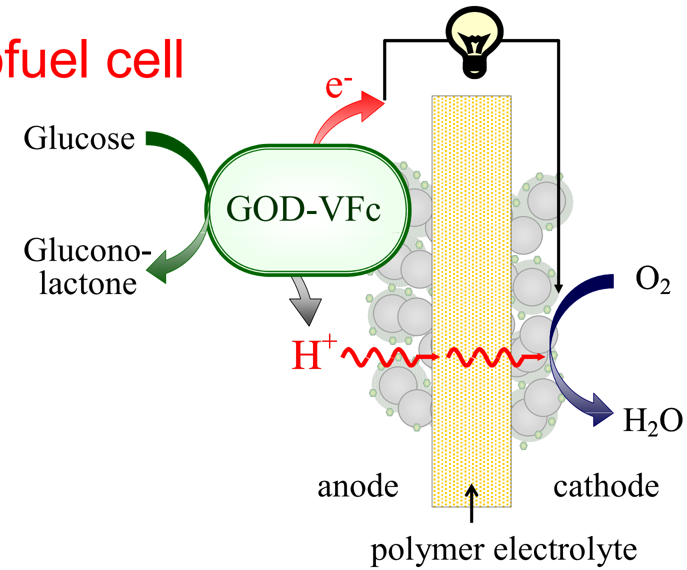

Center for Disease Biology and Integrative Medicine, Faculty of Medicine
Department of Chemical System Engineering, School of Engineering
Department of Bioengineering, School of Engineering
The University of Tokyo
Taichi Ito, Ph.D.

What is “system”？

System='integrated whole'

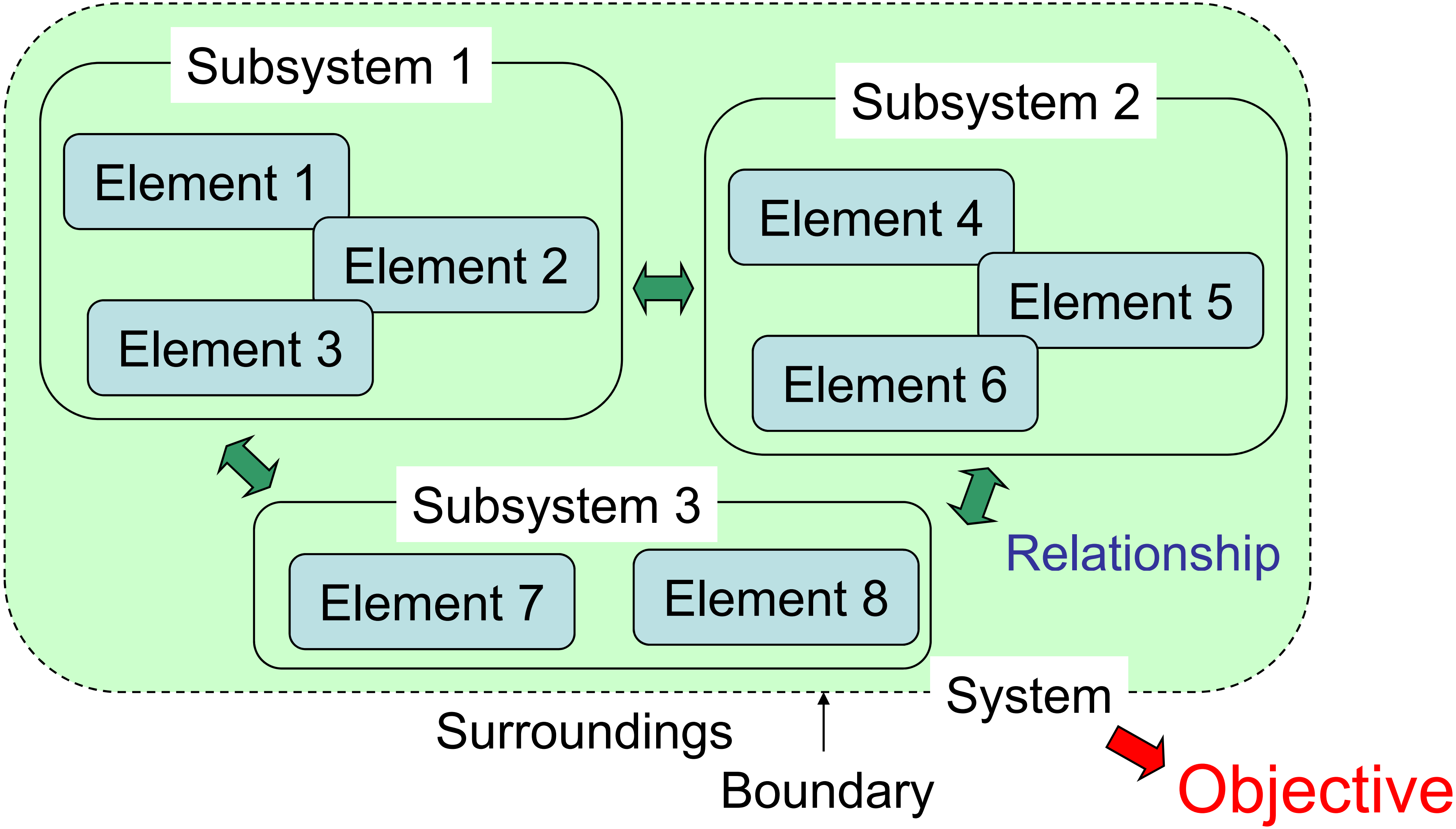

Living individual

System

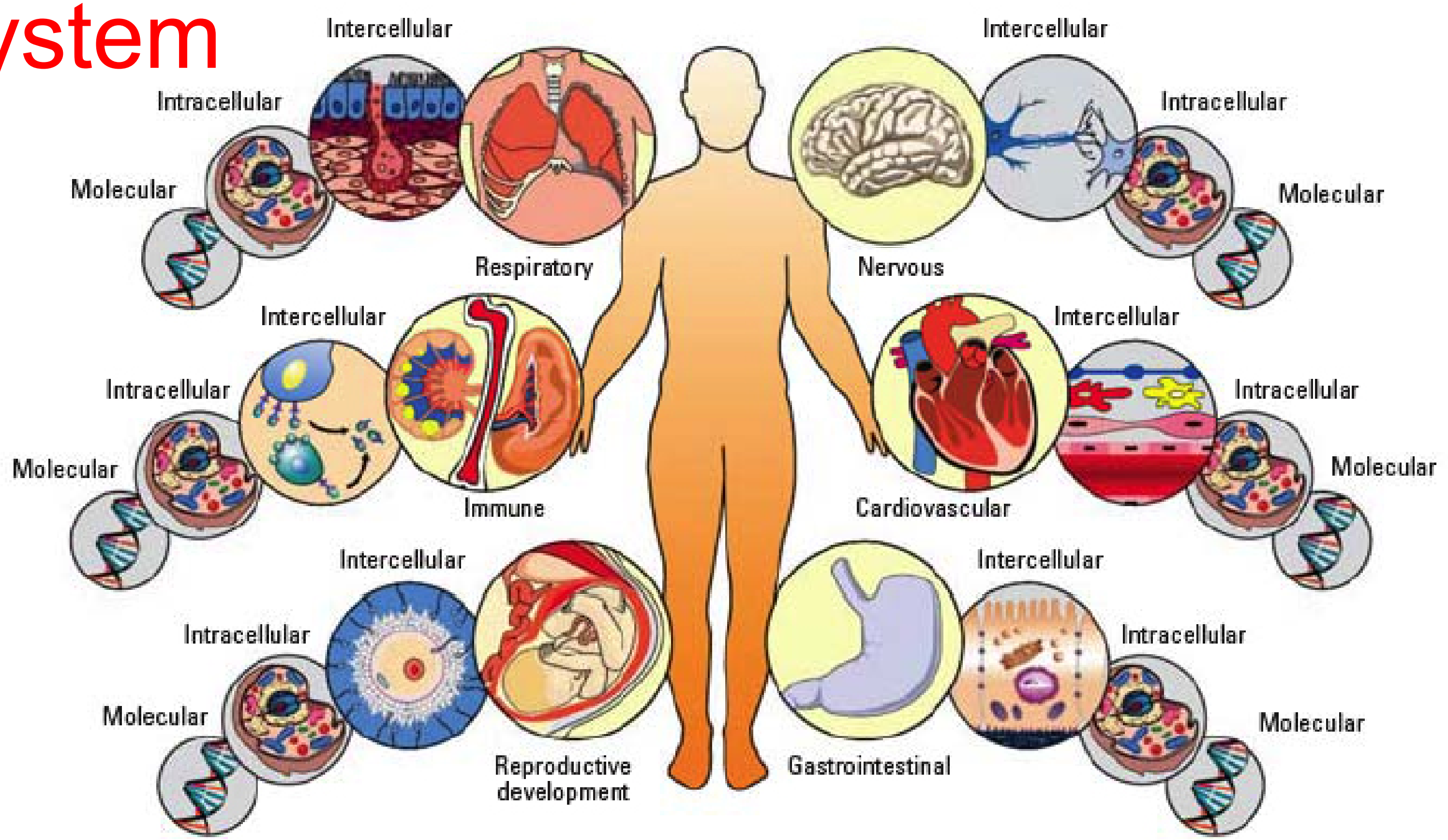

Figure 1. Systems biology framework for the individual. Current systems biology methodologies take advantage of high-throughput data generated at the molecular level in the hope of one day translating these maps of molecular interactions into cellular-level responses, then intercellular responses, and finally to an organ-level response. The interconnections between organ systems will need to be elucidated to understand an organism-level system.

http://ehp.niehs.nih.gov/members/2007/10373/fig1.jpg

Reverse engineering

the process of discovering the technological principles of a device, object or system through analysis of its structure, function and operation.

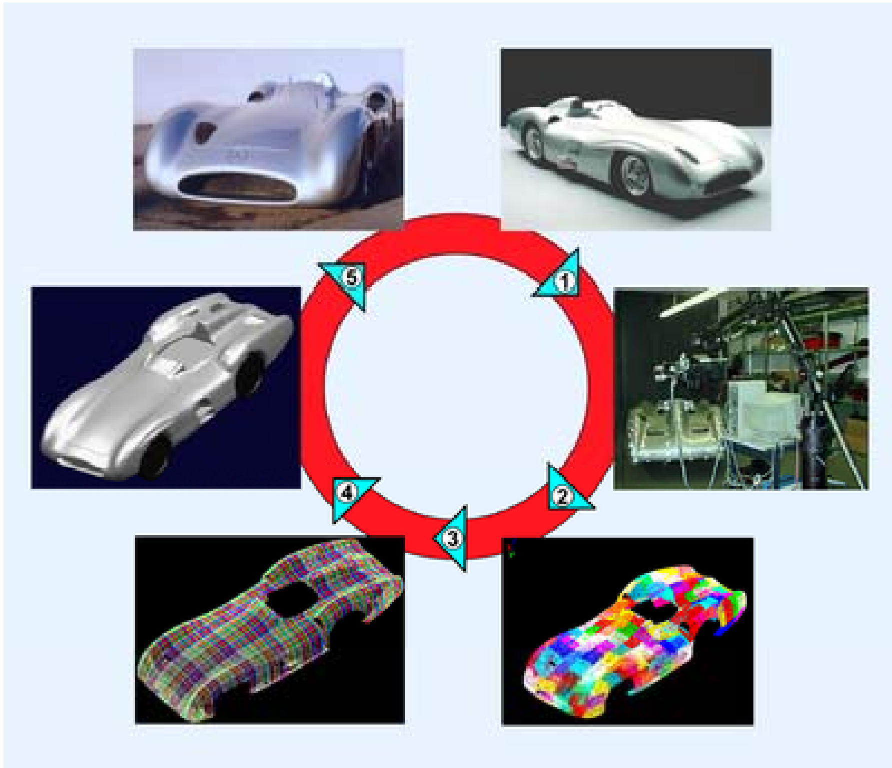

System Biology

Reverse engineering
of the living individual.

Inspired by
the principles
and functions

Design of new
artificial systems

Today's topics

Biosystems		*Inspired systems*
♣Ion channels	⇨	Molecular recognition ion gating membrane
♣energy metabolism	⇨	Biofuel cell

Artificial membrane

Separation membrane

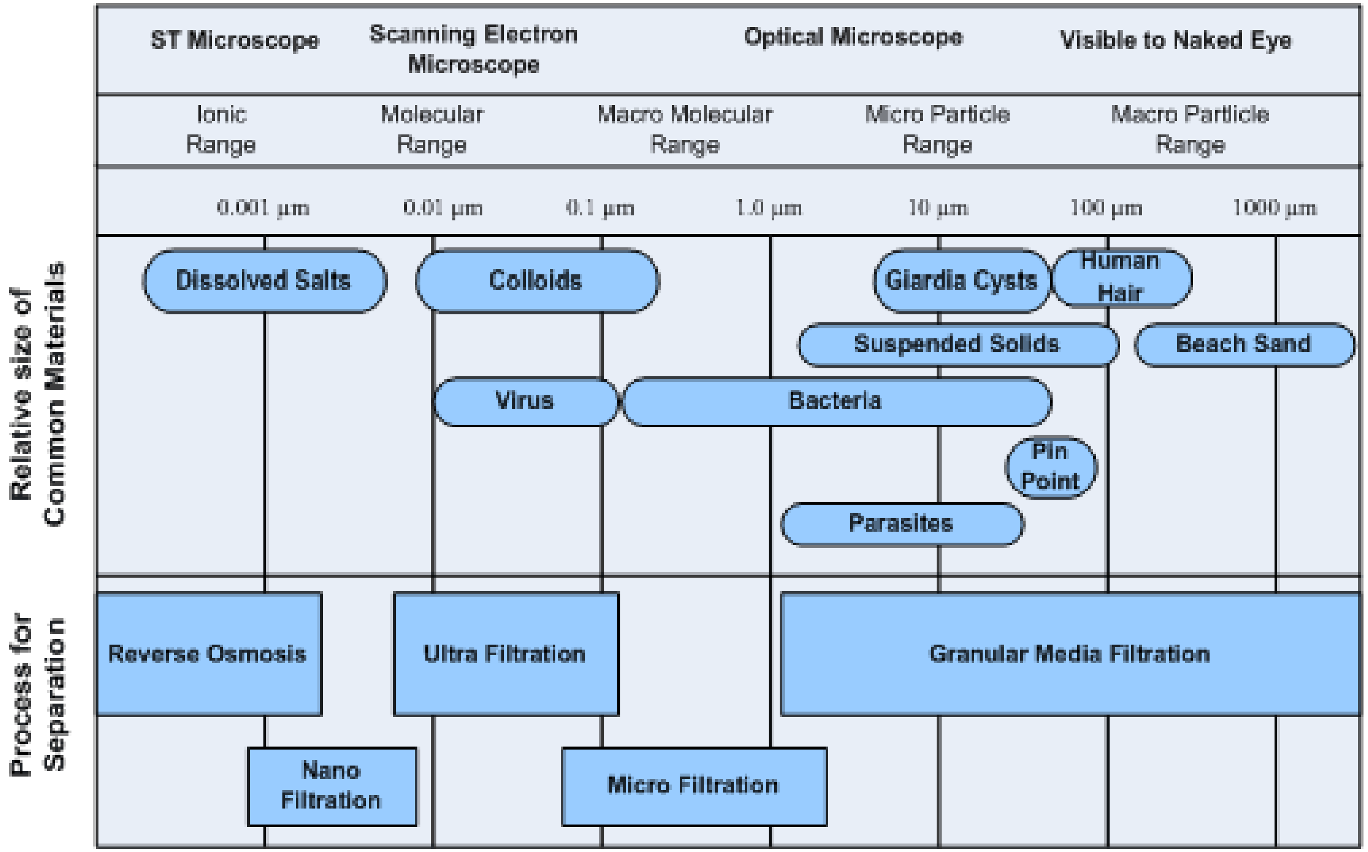

http://www.actew.com.au/water2water/MicrofiltrationandUltrafiltration.aspx

Ultra filtration and micro filtration

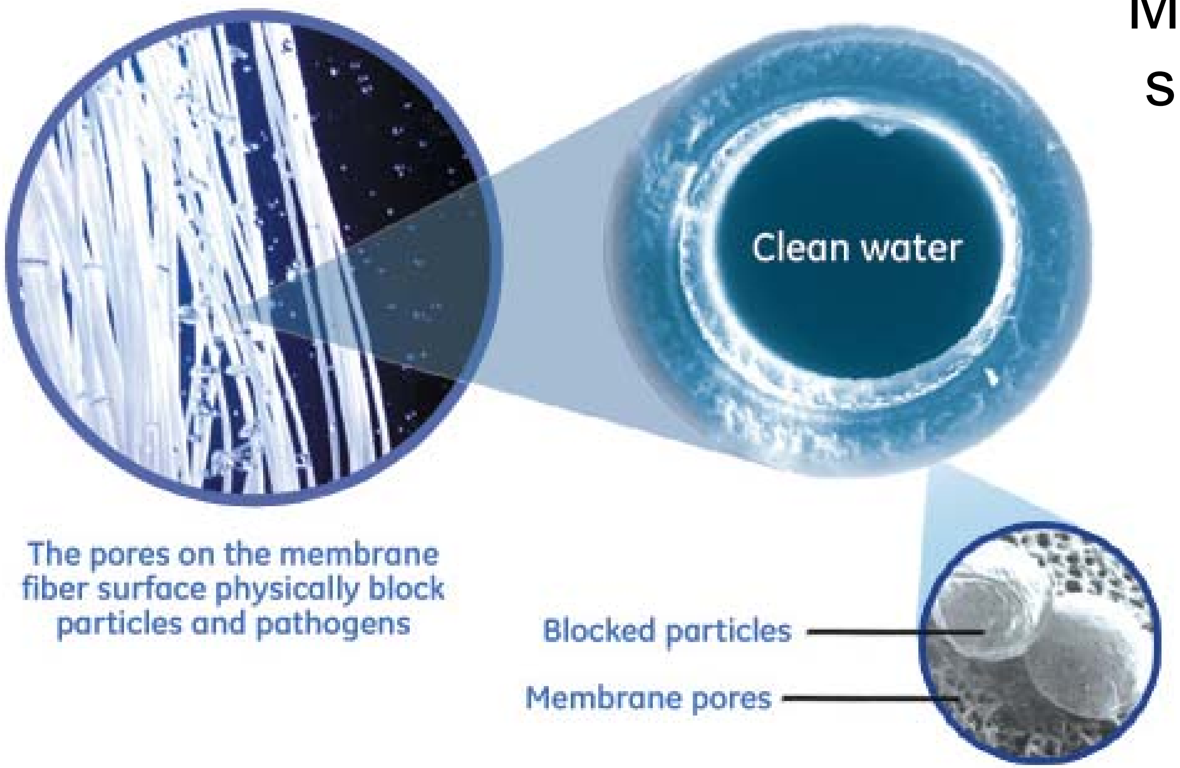

Molecular or particle sieving by the pores

http://www.homespring.com/how_it_works.shtml

Biomembrane

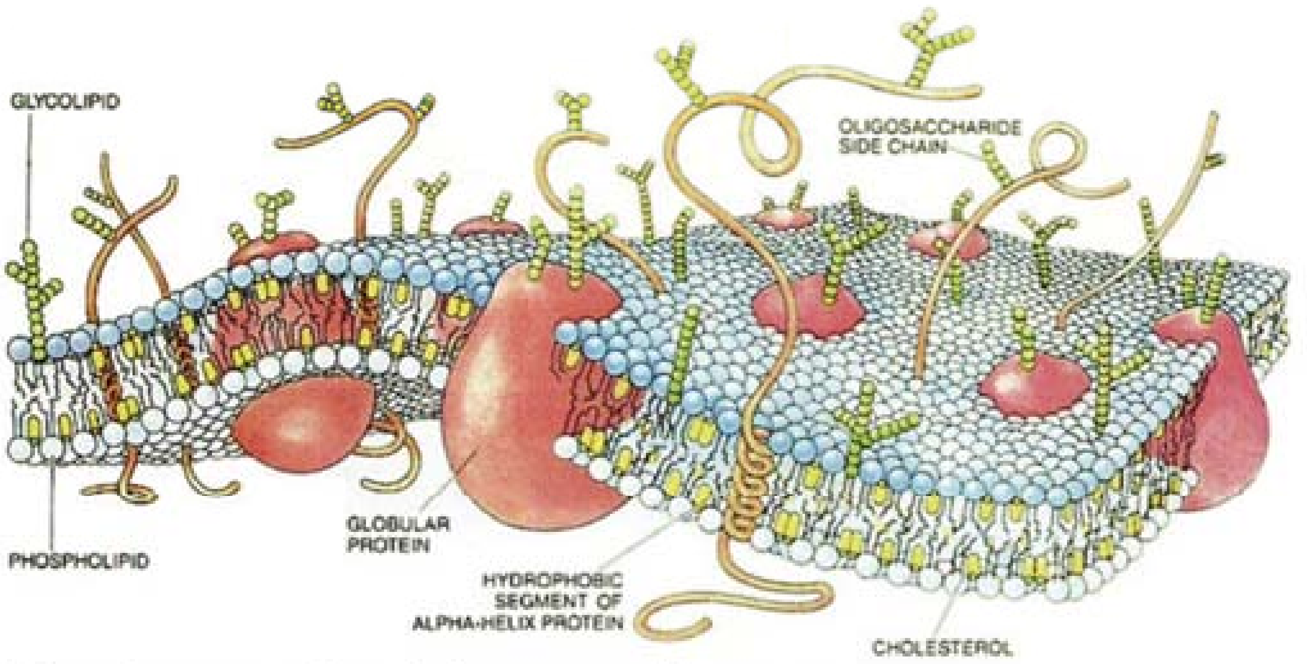

Cartoon of a biomembrane

http://www.cmu.edu/biolphys/smsl/

Ion channel

molecular structure of potassium channels

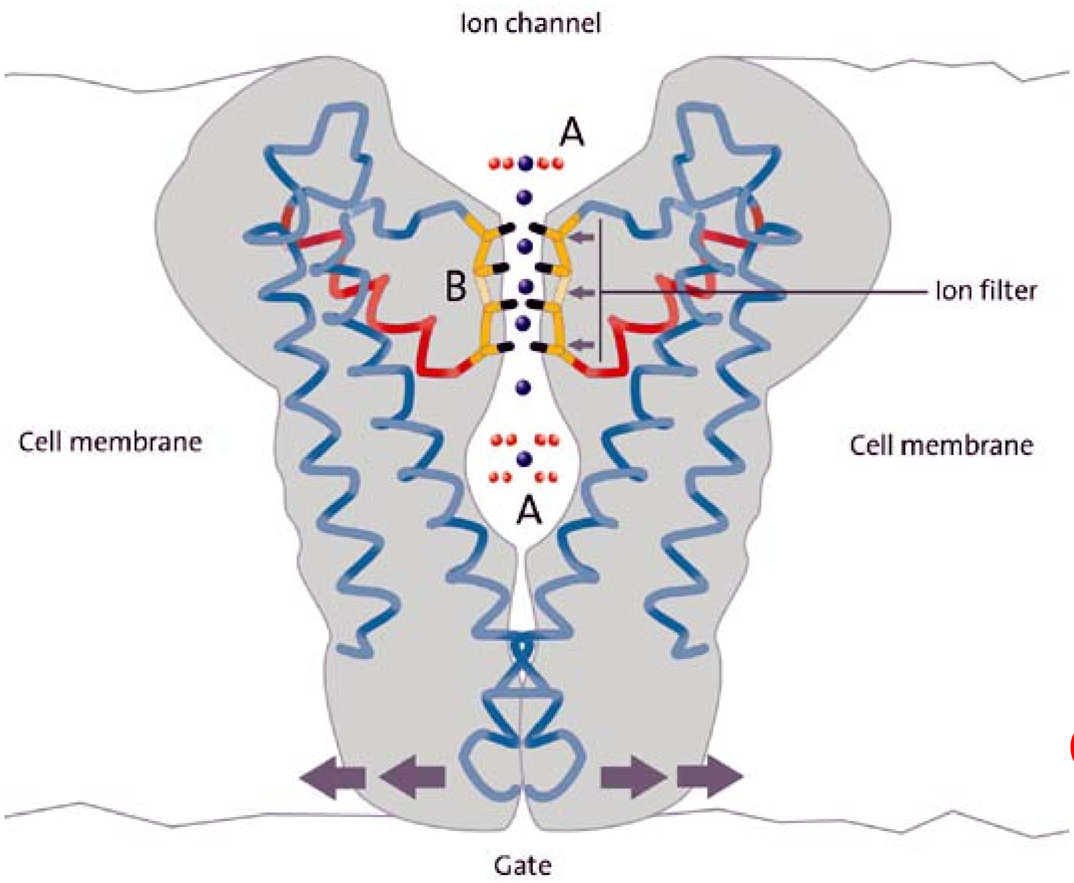

K⁺ filter

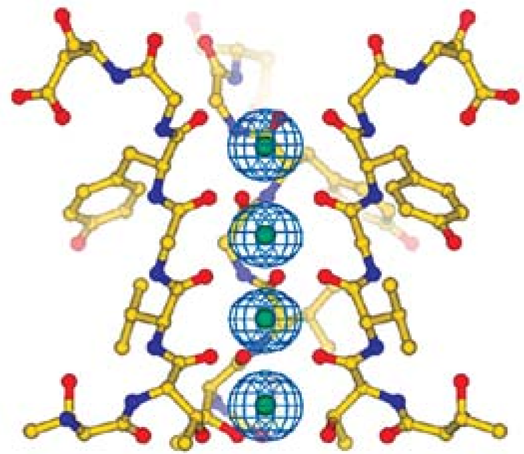

Nature2001
João H. Morais-Cabral, Yufeng Zhou and Roderick MacKinnon
Energetic optimization of ion conduction rate by the K+ selectivity filter

Can we make an artificial ion channel?

Ion Recognition Polymer

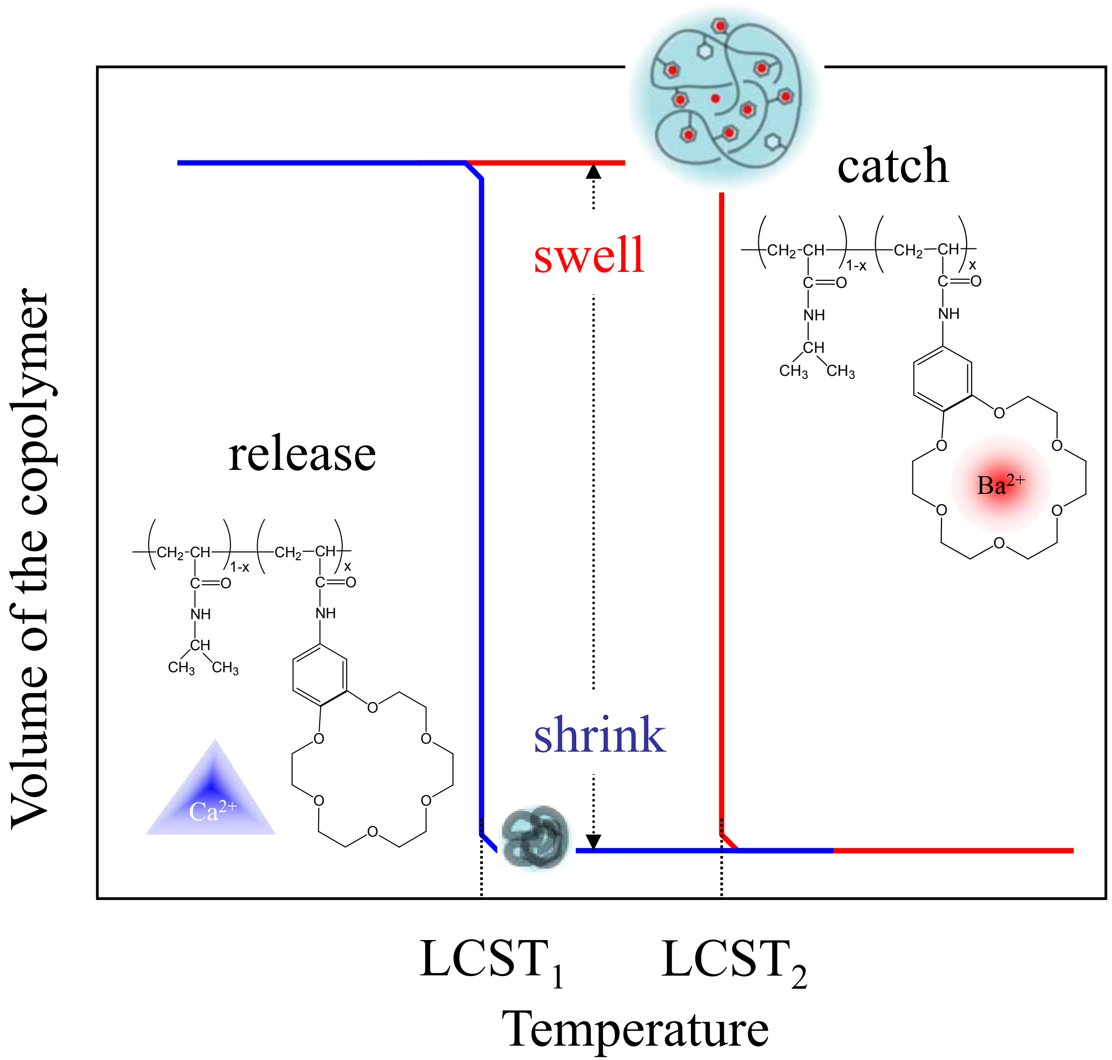

Capture of ions

LCST (Lower critical solution temperature) shifts to higher temperature.

At a constant temperature, polymer swells and shrinks in response to specific ion concentration change.

Irie *et al.Polymer* 1993(34)4531

Molecular Recognition Ion Gating Membrane

Ion recognition polymer

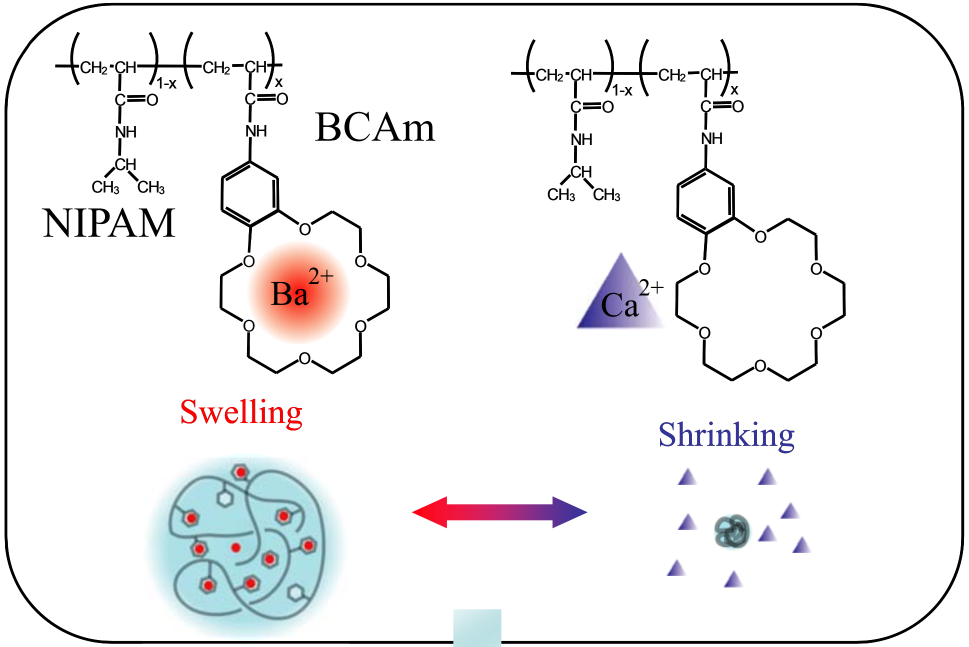

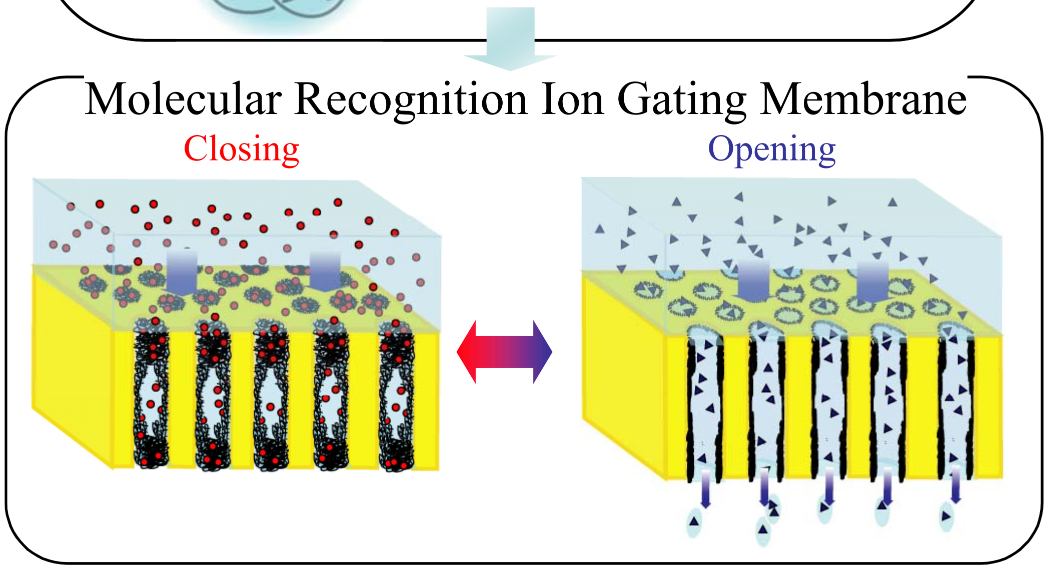

Crown Receptors
capture ions.

↓

Grafted polymer swells.

↓

Pores close.

Crown receptors
does not capture ions.

↓

Grafted copolymer shrink.

↓

Pores open.

Preparation of the membrane

Porous substrate

Graft polymerization

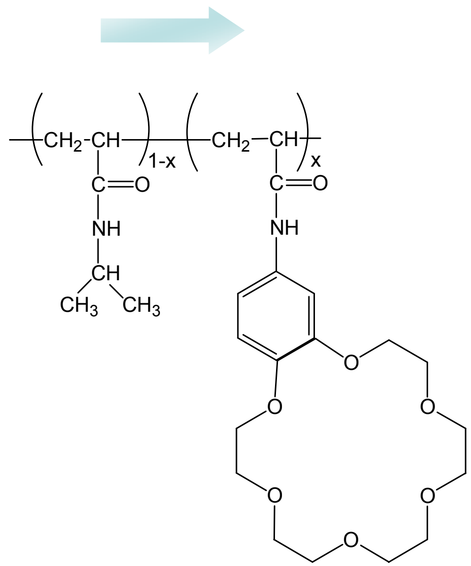

Small grafting amount

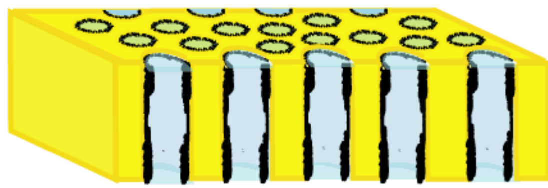

Large grafting amount

Molecular recognition
ion gating membrane

Plasma graft polymerization

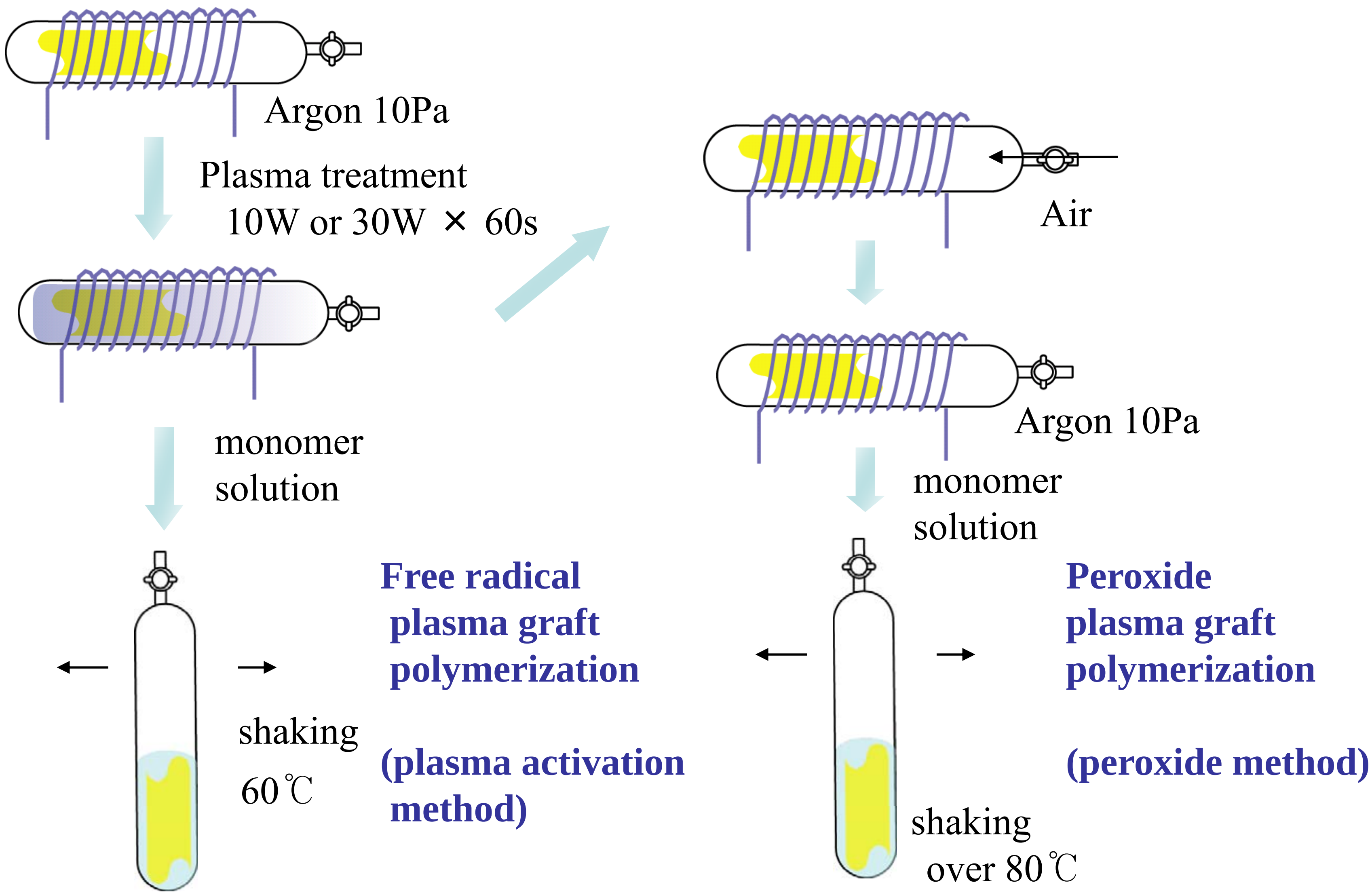

IR spectra

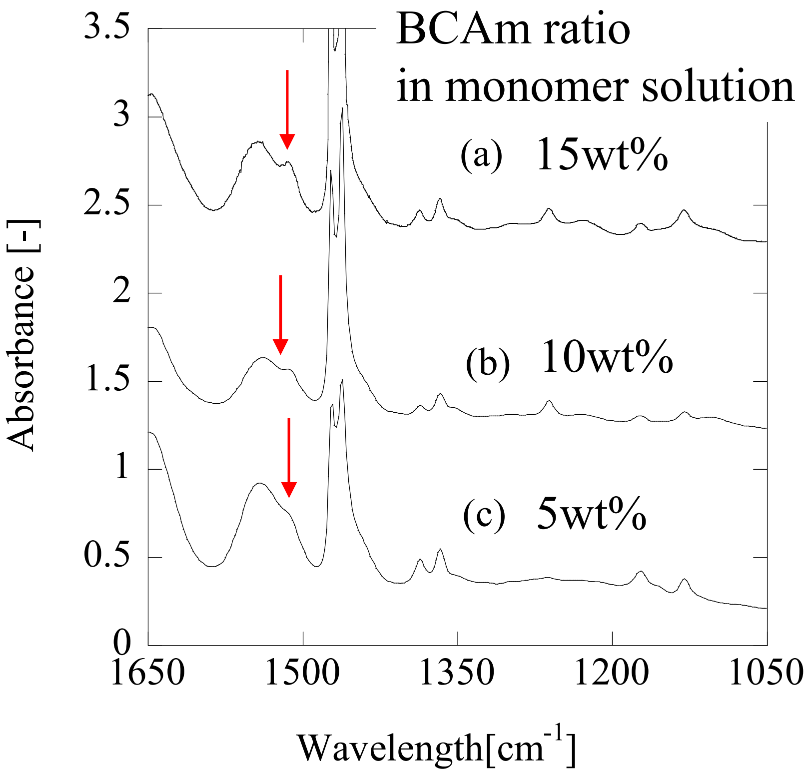

FT-IR spectra of PE-g-NIPAM-co-BCAm prepared by the peroxide plasma graft copolymerization. The weight percentage of BCAm in the total monomer were (a)15wt%, (b)10wt%, and (c)5wt%,respectively.

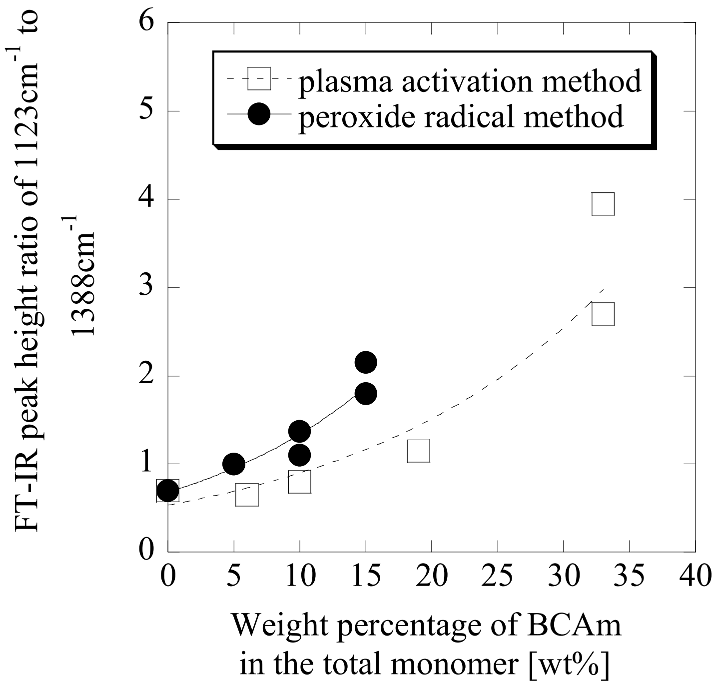

. FT-IR peak height ratio of $1123cm^{-1}$ to $1388cm^{-1}$ of PE-g-NIPAM-co-BCAm. The $1388cm^{-1}$ and $1123cm^{-1}$ peak represents isopropyl group of NIPAM and ether group of BCAm, respectively. The peroxide radical method grafted more BCAm monomer than the plasma activation method from the same monomer solution.

The grafted membrane surface

FE-SEM observation

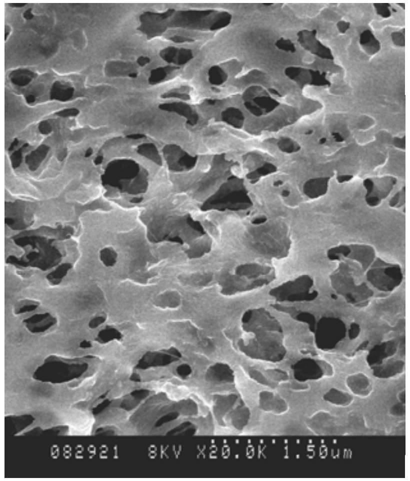

Substrate
(grafting ratio: 0%)

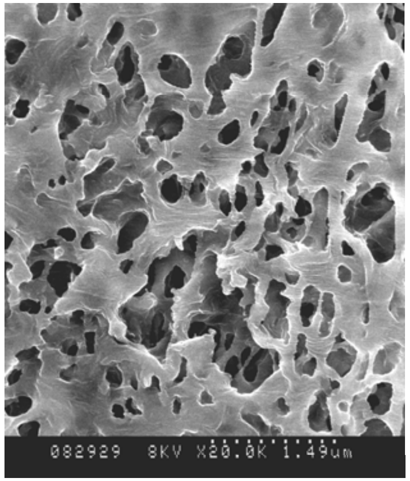

0.45mg/cm^2
(6.5%)

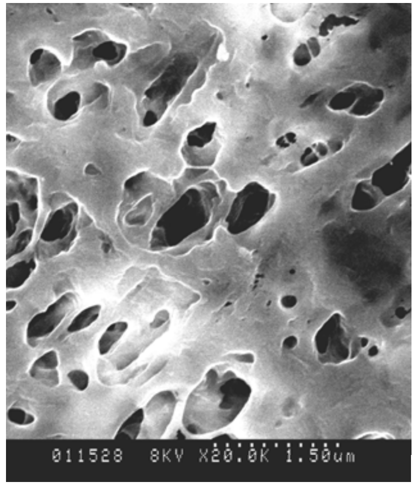

0.72mg/cm^2
(10.4%)

$$\text{grafting ratio} = \frac{\text{grafted polymer volume}}{\text{grafted polymer volume}}$$

Filtration control functions

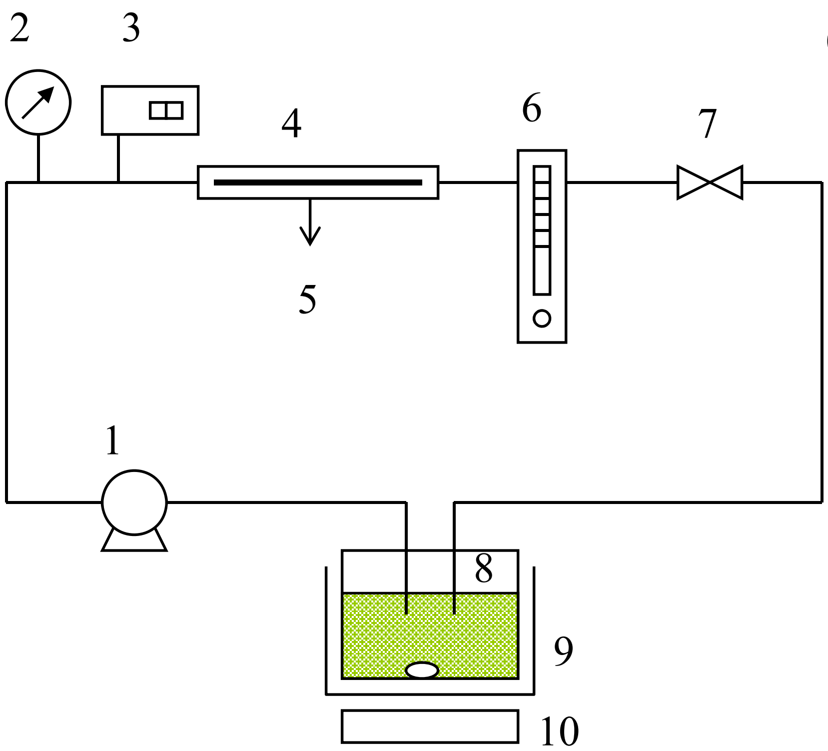

1.Pump 2.Pressure gauge 3.Thermometer 4.Test cell
5.Permeation solution 6.Flow meter 7.Pressure valve
8.Feed Tank 9.Thermostat 10.Stirrer

Cross-flow filtration experiments

<u>Aqueous ion solution</u>

$BaCl_2$, $SrCl_2$, $CaCl_2$
$PbCl_2$, KCl, NaCl, LiCl

<u>Aqueous ion and ethanol solution</u>

<u>Aqueous ion and dextran solution</u>

Temperature change
Concentration change
Response rate
Rejection control

LCST shift in response to ion signal

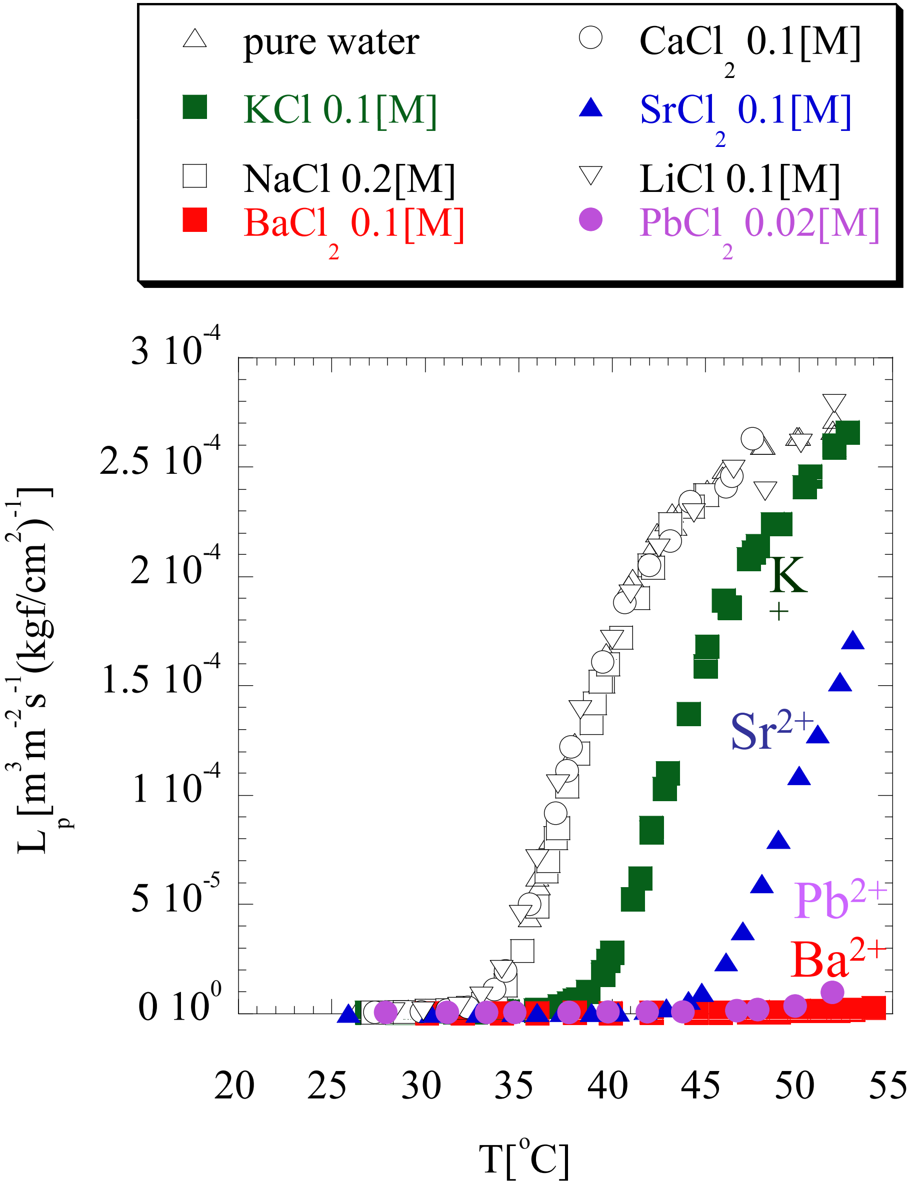

Log K of Benzo[18]crown-6

Ion	LogK (poly-BCAm-co-NIPAM)	LogK (Benzo[18]crown-6)
Ba^{2+}	**1.6**	2.90
Sr^{2+}	**1.1**	2.41
K^+	**1.0**	1.74

LCST shifted to higher temperature in response to specific ions.

Ion concentration response

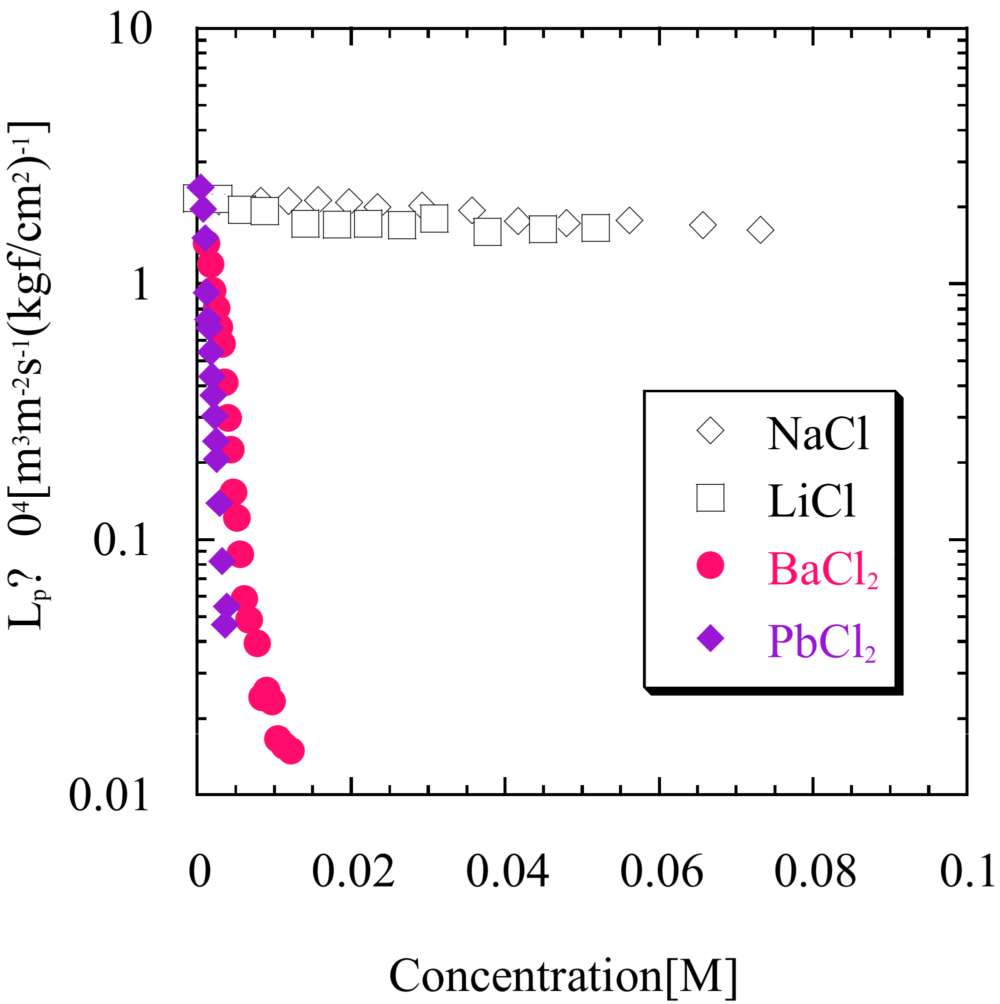

At a constant temperature

Pores closed in response to specific ion concentration change.

Molecular recognition ion gating membrane

Response rate and reversibility

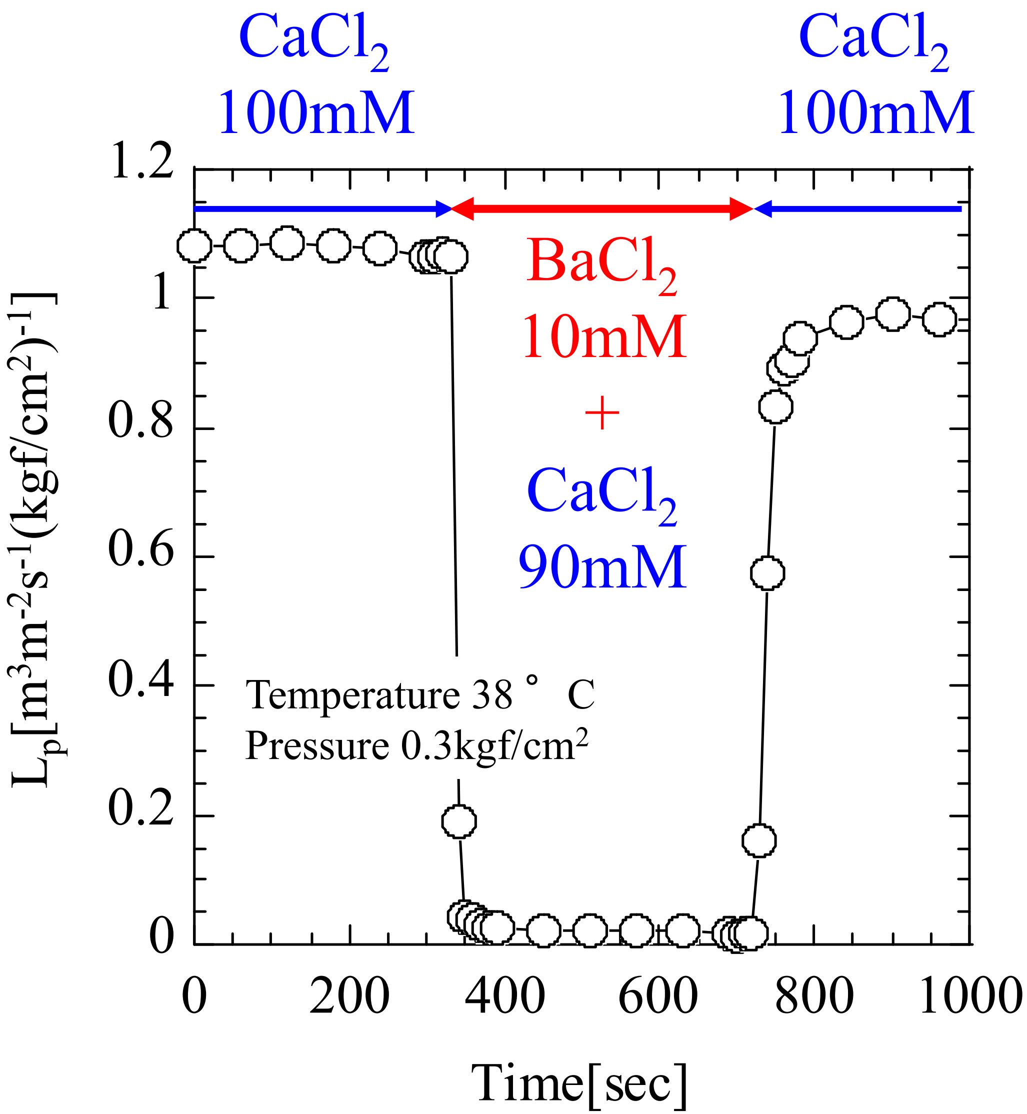

Crosslinked hydrogel

Responding hour: several hours

High response rate several seconds

Response reversibility

Control of separation function

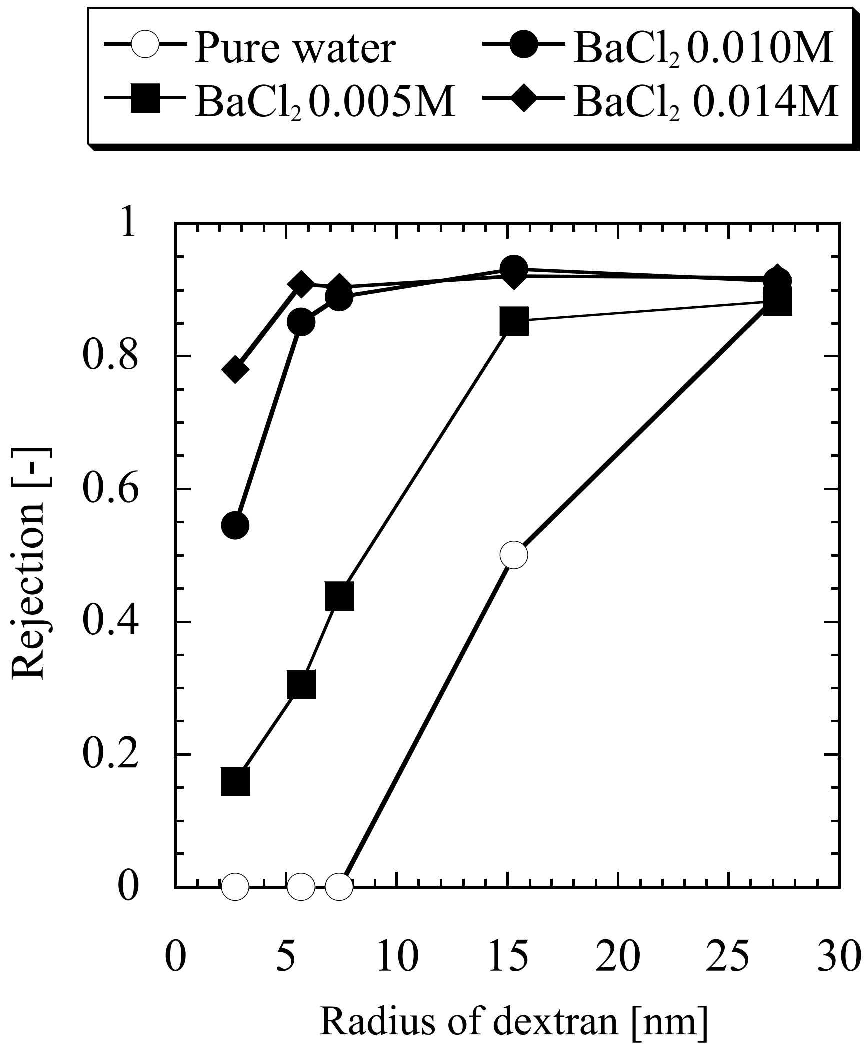

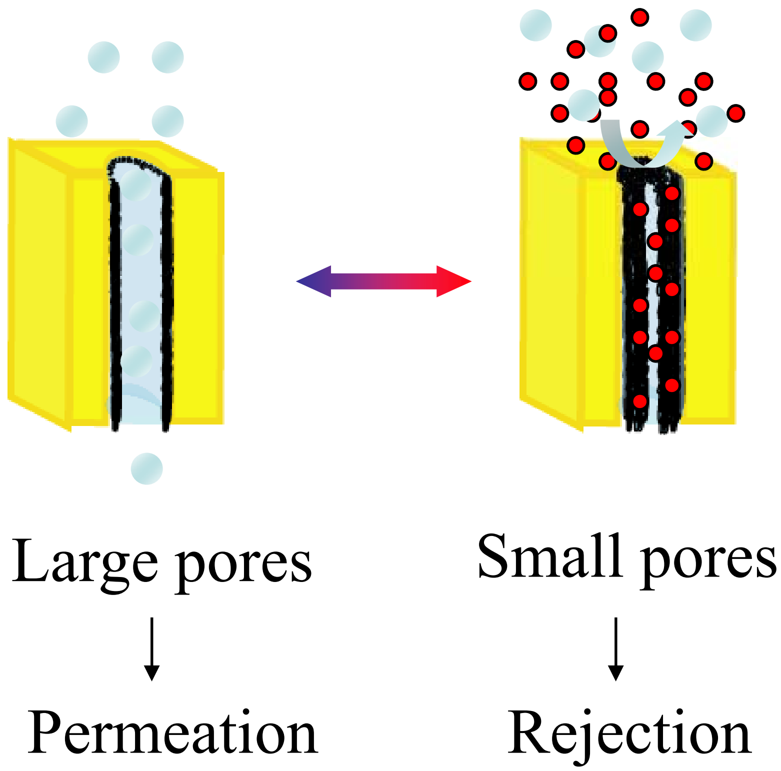

Control of separation function in response to signal ion concentration.

Osmotic pressure control functions

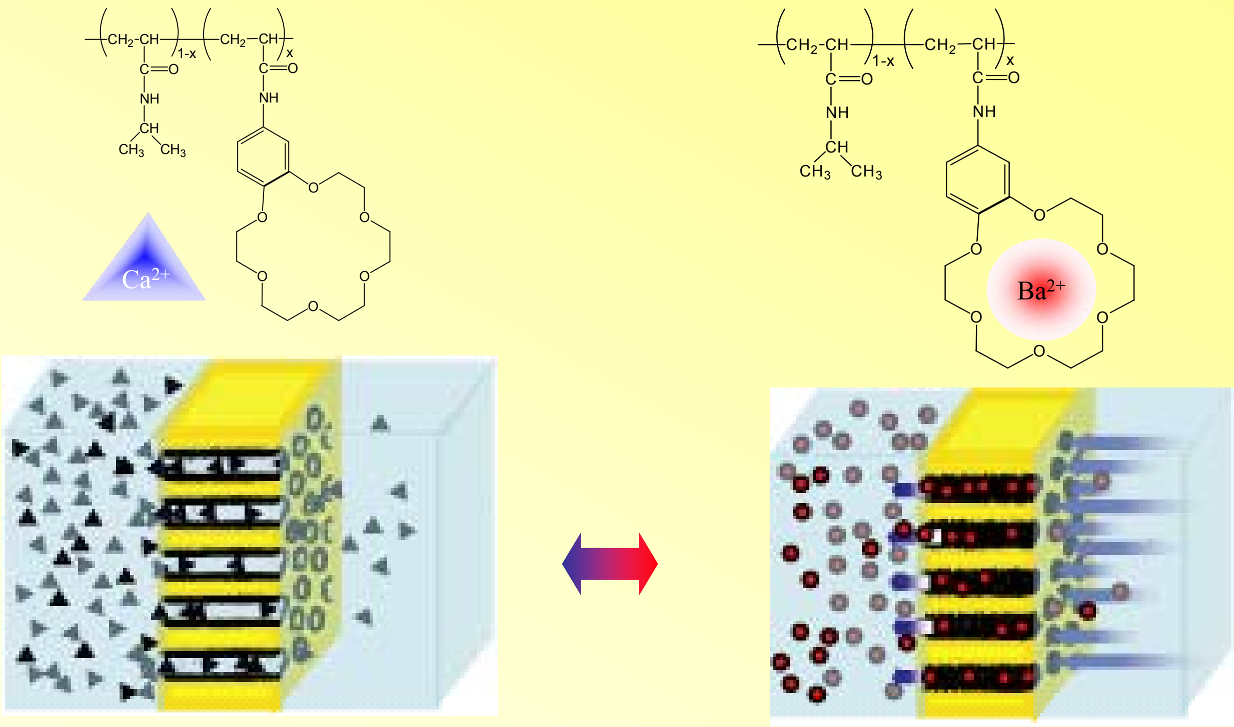

Opening of pores | Closing of pores

- ·Osmotic pump type DDS
- ·Actuator

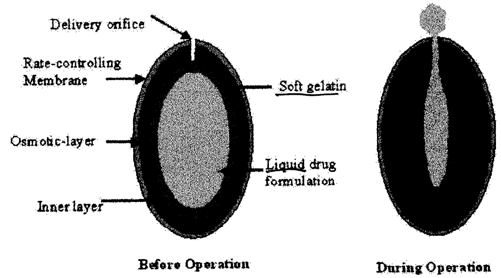

Cross-sectional diagram of L-OROS delivery system before and during operation. Courtesy by Alza Corp., reprinted from Ref. [11] with permission of the Controlled Release Society 2000©.

Experiment

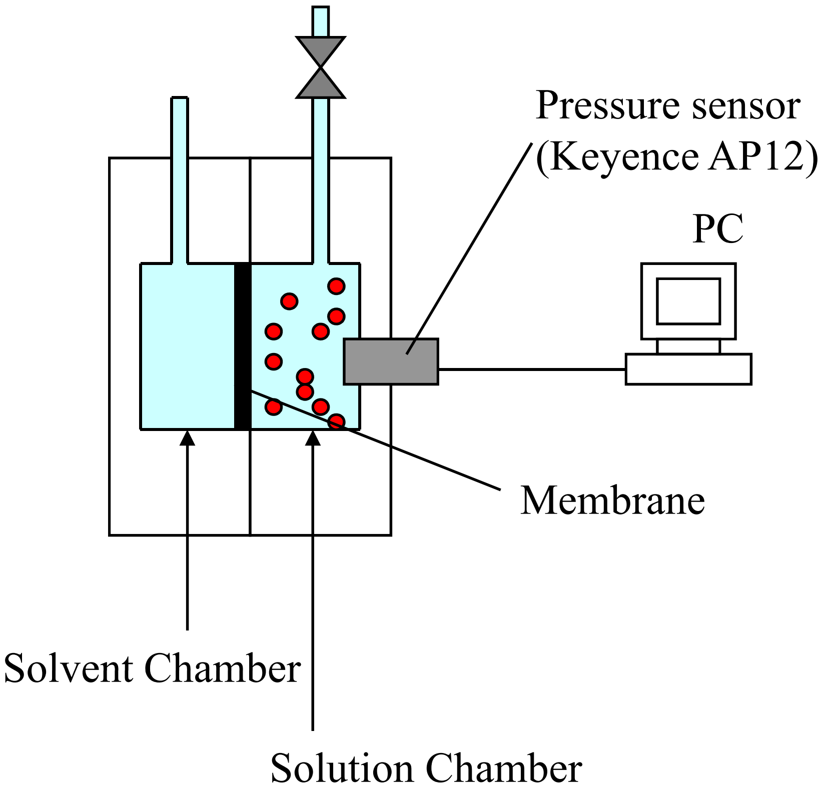

Solution

<u>Aqueous solution</u>

$BaCl_2$, $CaCl_2$, $SrCl_2$
NaCl, KCl

<u>Aqueous ion and dextran solution</u>

dextran T500,T70,4
$BaCl_2$, $CaCl_2$

Membrane

Grafting ratio 14.6%

Osmotic pressure generated by ion concentration gradient

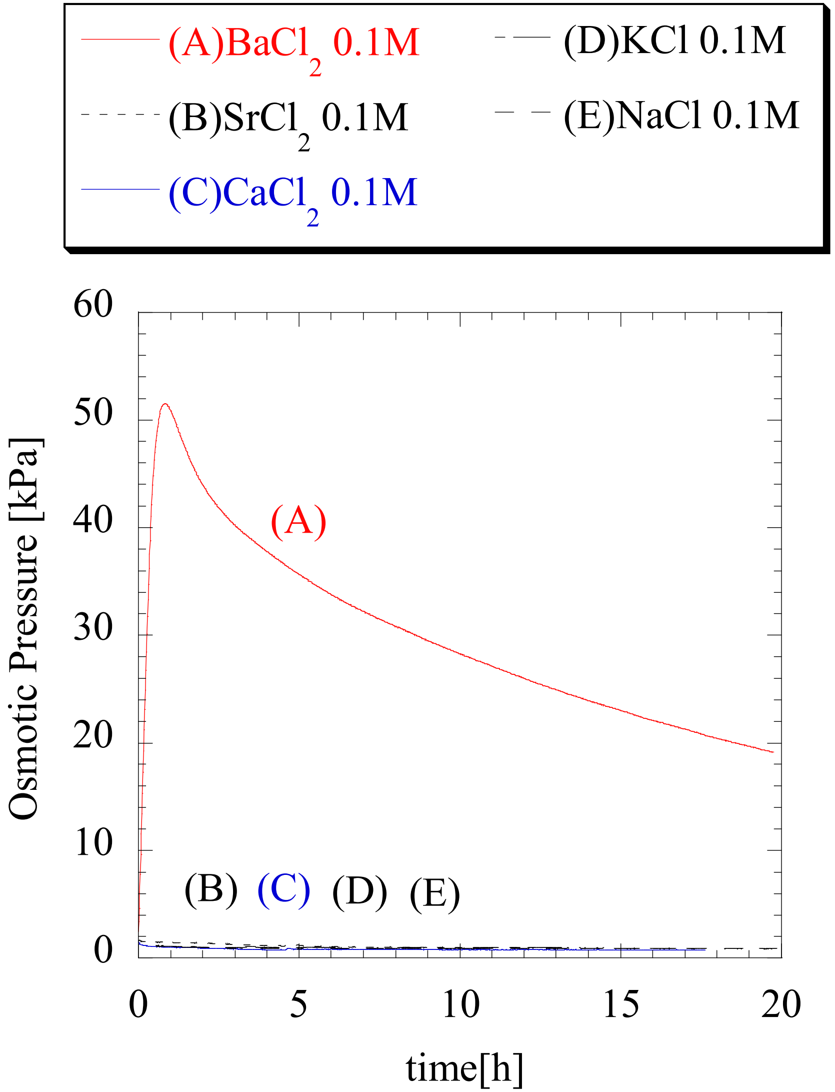

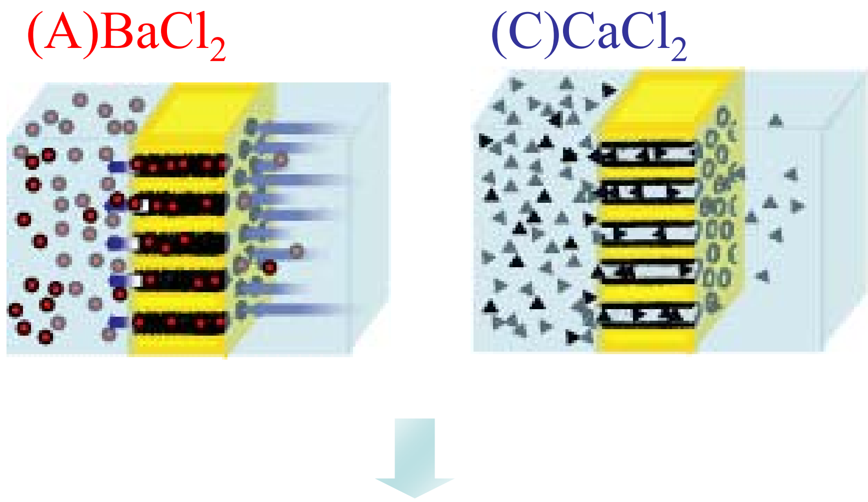

Osmotic pressure generation in response to a specific ion

Osmotic pressure decreased owing to decrease of concentration gradient with diffusion.

Reversibility

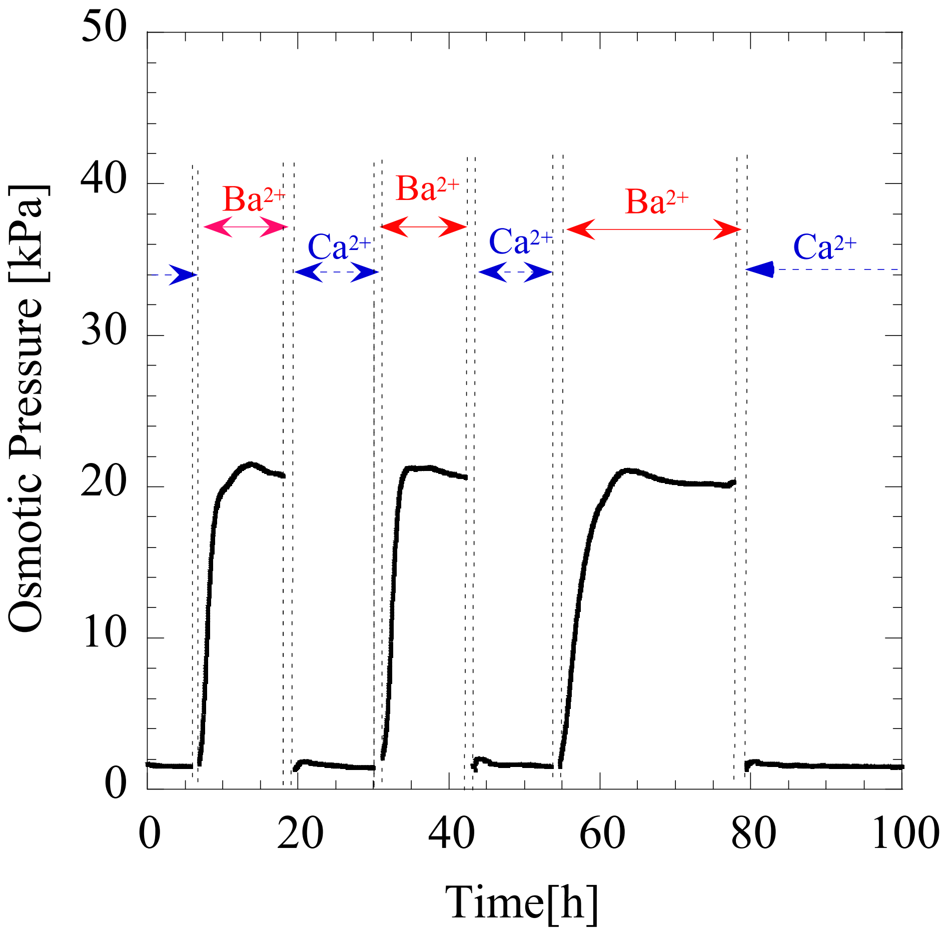

dextranT500 0.1g/ml
Ion concentration 0.1M
Temperature 39.0° C constant

Osmotic pressure occurred repeatedly in response to Ba^{2+}.

Utilization of pulsatile release in response to an ion signal.

What do K+ channels work in biosystems?

Self-excited nonlinear oscillation of biomembrane

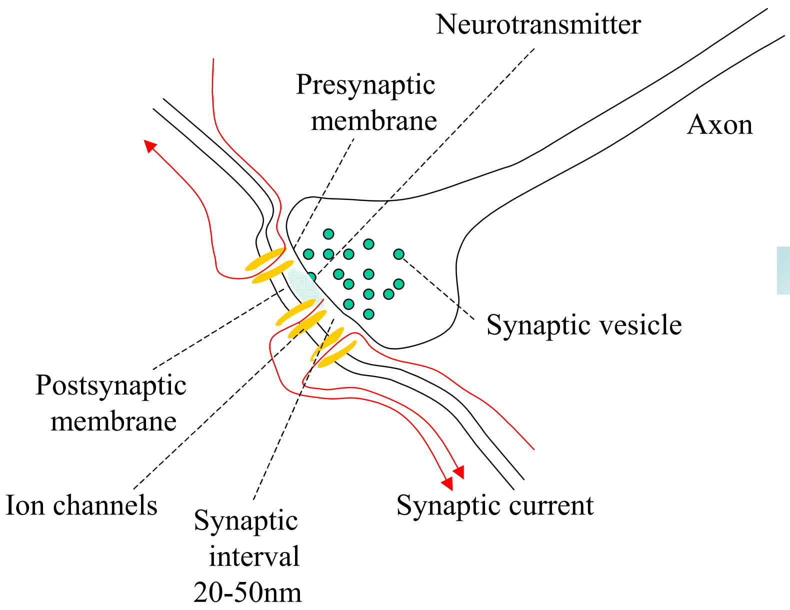

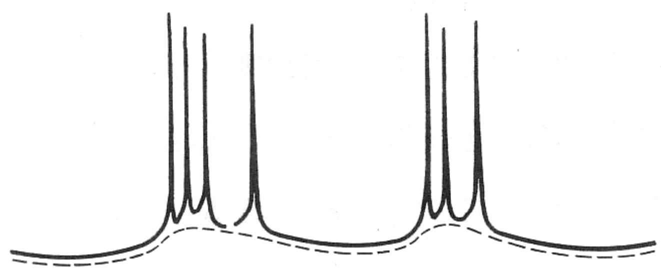

Spontaneous discharge of
Peronia verruculata neuron
(Hayashi et al. J. Theor.Biol. 1992)

Nonlinear self-excited ion recognition oscillator

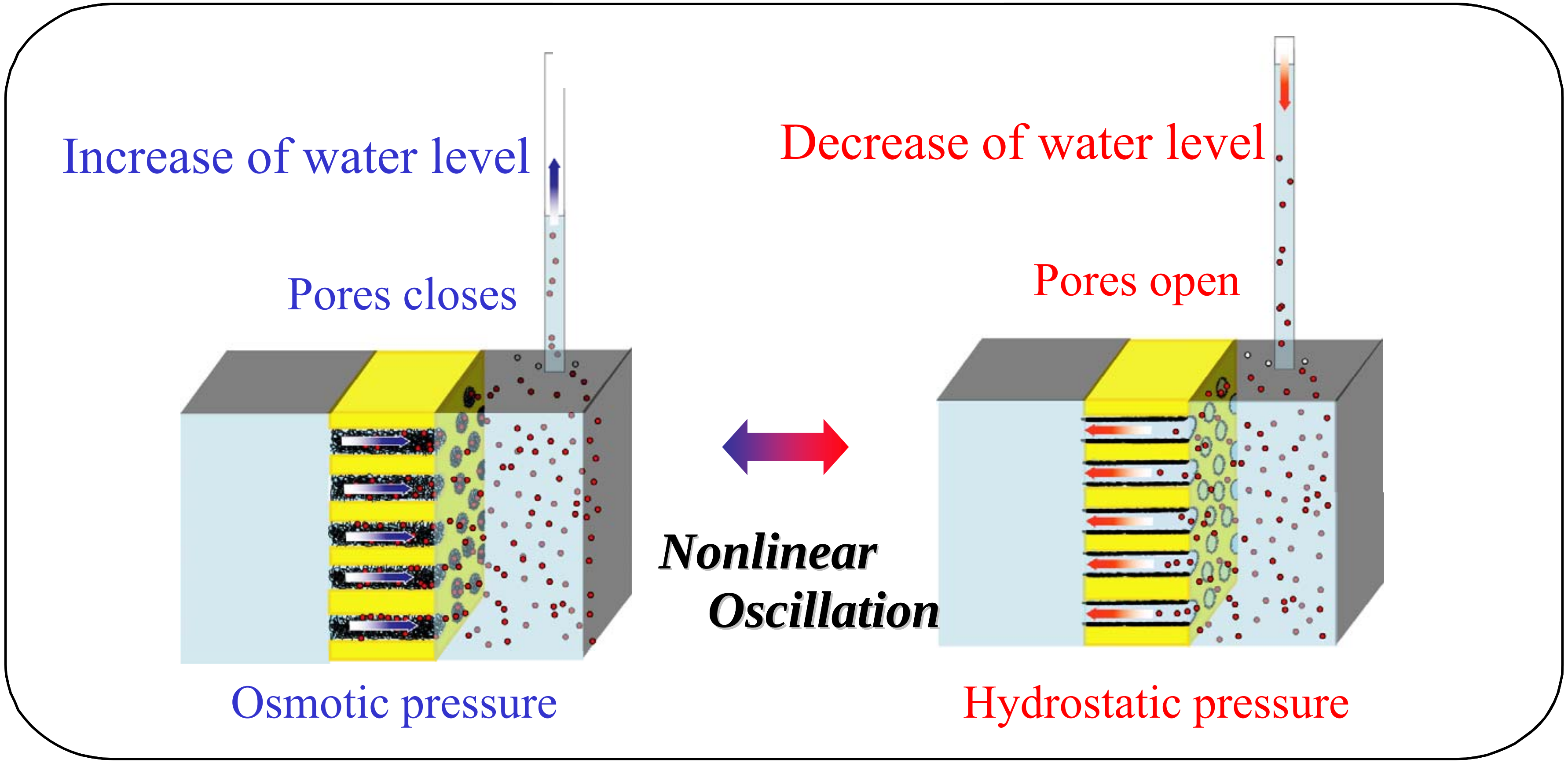

Pores open and close autonomously and repeatedly.

Bistability of hydrostatic-pressure driven flow and osmotic-pressure driven flow

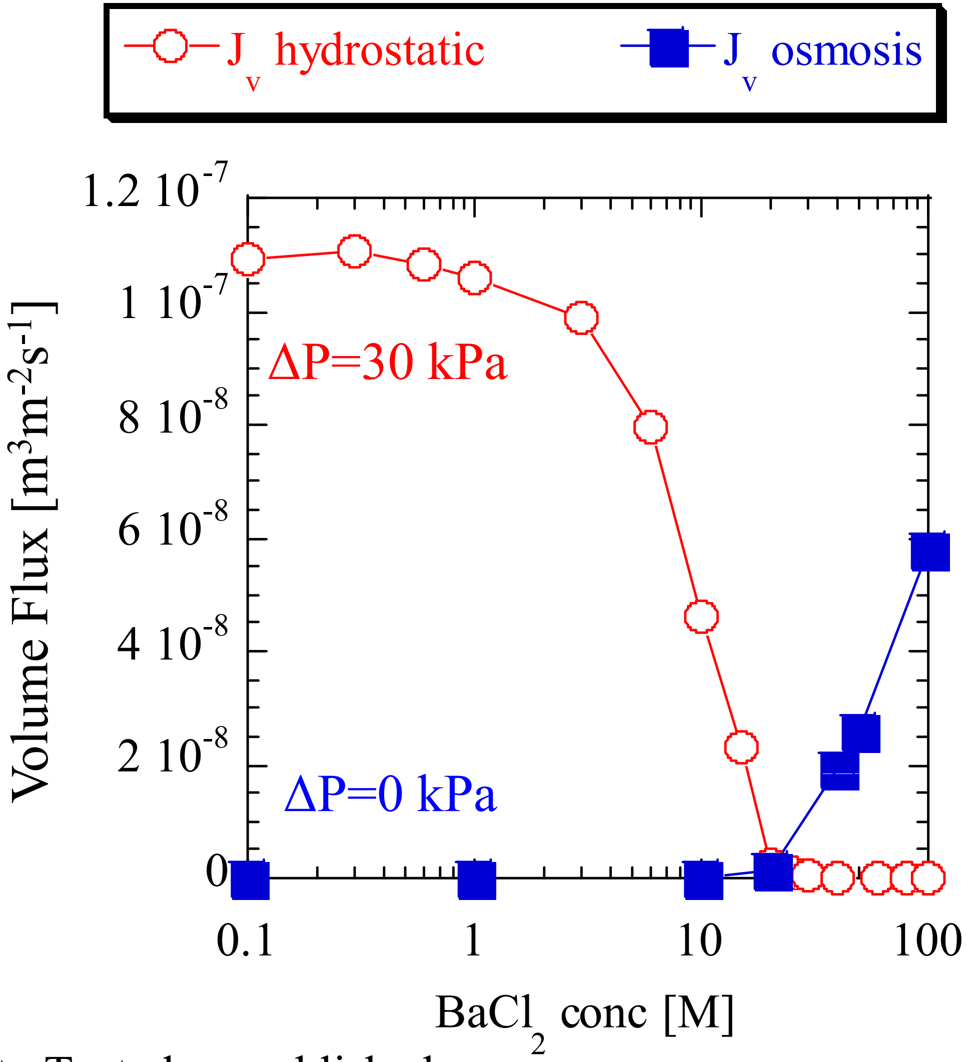

Ito,T. et al. unpublished

$BaCl_2$ < 20mM

Hydrostatic pressure-driven flow

Down-flow

$BaCl_2$ > 20mM

Osmotic pressure-driven flow

Up-flow

Bistablility at about 20mM

Waveform

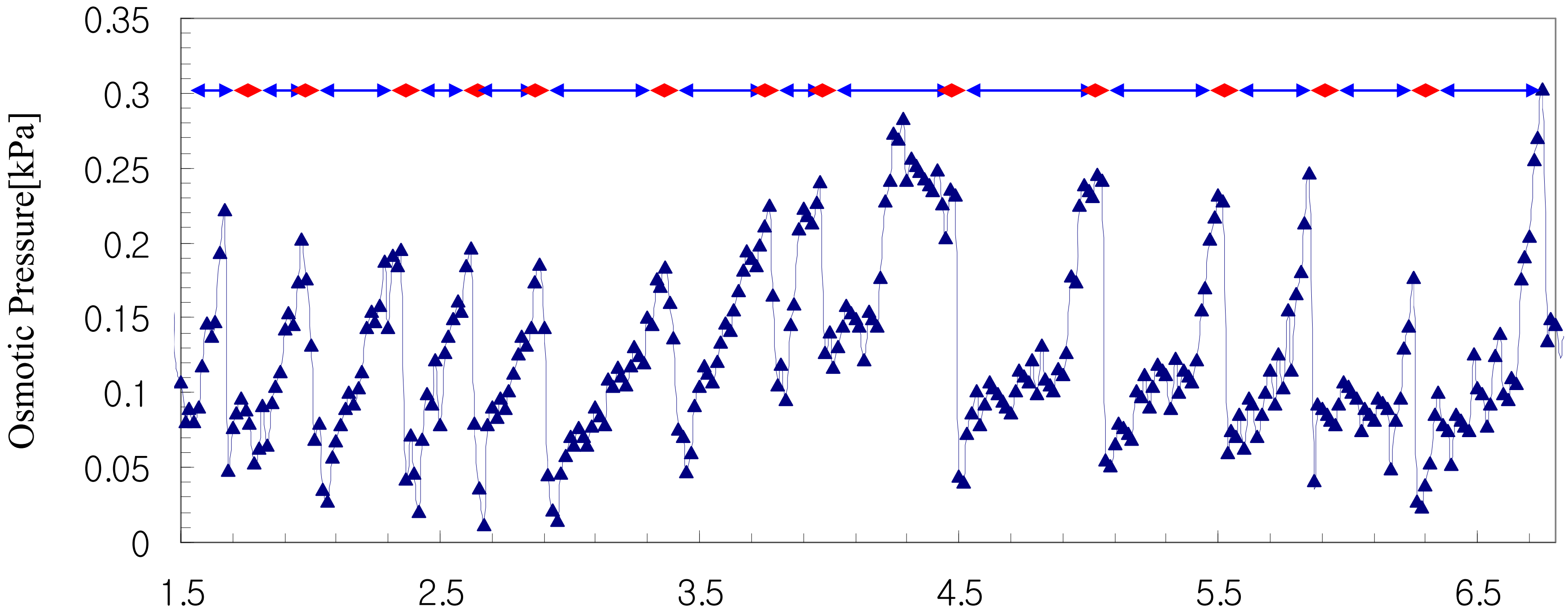

Change of waveform

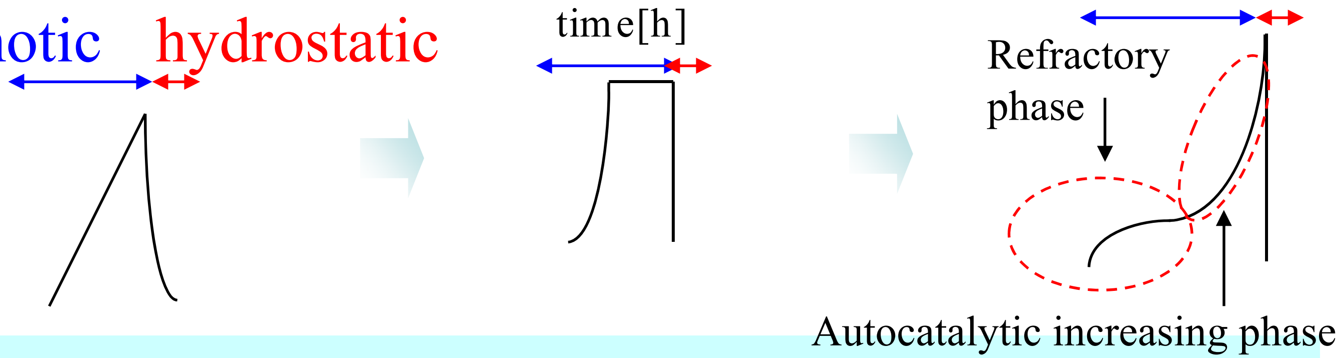

Combination of fast mode and slow mode

<u>relaxation oscillation</u>

Mathematical modeling of ion recognition oscillation

"Shishiodoshi"

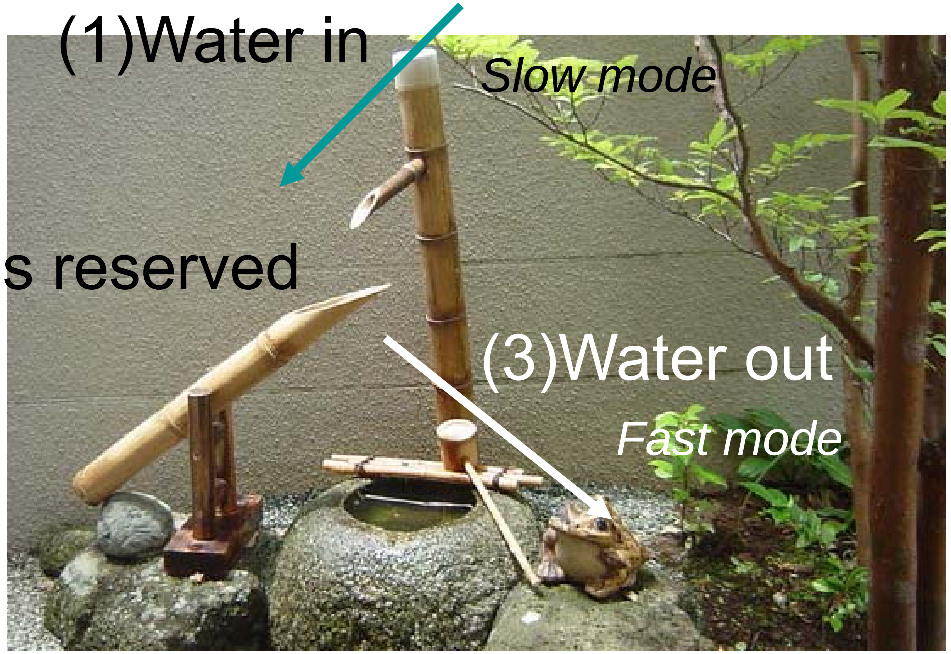

Relaxation oscillation

slow mode with energy accumulation + fast mode with energy release

Equation of state

$$V\frac{dc}{dt} = A(1-\sigma)(c_{in} - c)L_p\left|(\Delta P - \sigma\Delta\Pi)\right|$$

$$\frac{ca}{g}\frac{d(\Delta P)}{dt} = -maL_P(\Delta P - \sigma\Delta\Pi)$$

$$\frac{d\sigma}{dt} = \frac{1}{\tau_\sigma}(\sigma_\infty - \sigma)$$

$$\frac{dL_p}{dt} = \frac{1}{\tau_{L_p}}(L_{p\infty} - L_p)$$

$$L_{p\infty} = L_0\left(1 - \frac{(\frac{c}{c_1})^n}{a + (\frac{c}{c_1})^n}\right)$$

$$\sigma_\infty = \sigma_0\frac{(\frac{(c-c_3)}{c_2})^m}{b + (\frac{(c-c_3)}{c_2})^m}$$

First order simultaneous ordinary differential equation

Phenomenological equations

+

Saturation type nonlinear-character + Time lag

Numerical calculation
By Runge-Kutta method

Water level

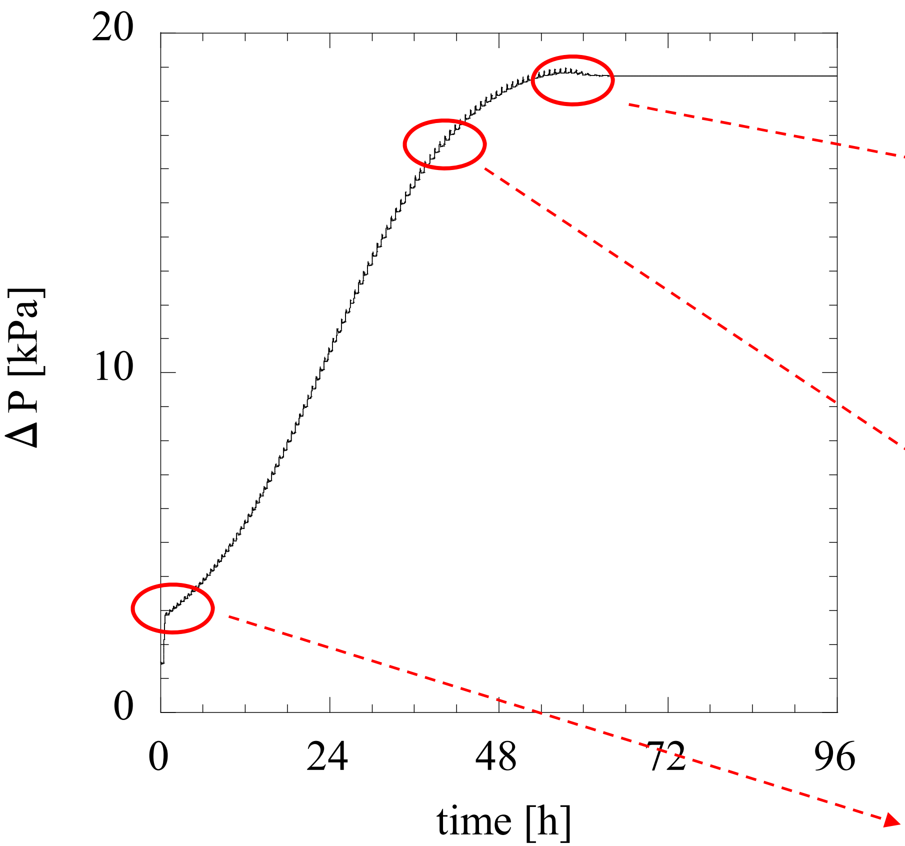

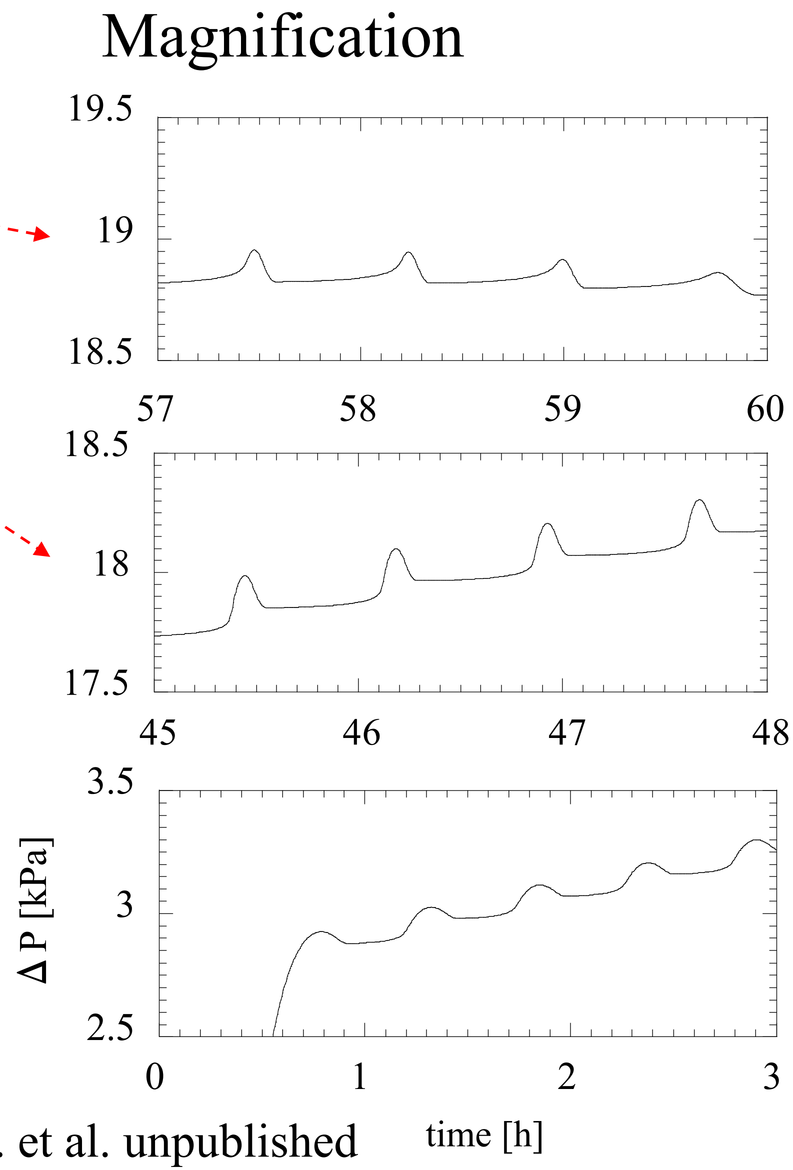

Reproducde periods and amplitudes by numerical calculation

Ito,T. et al. unpublished

Temperature-responsive cell culture dish

NIPAM-grafted culture dish

Confluent

Detachment of cells

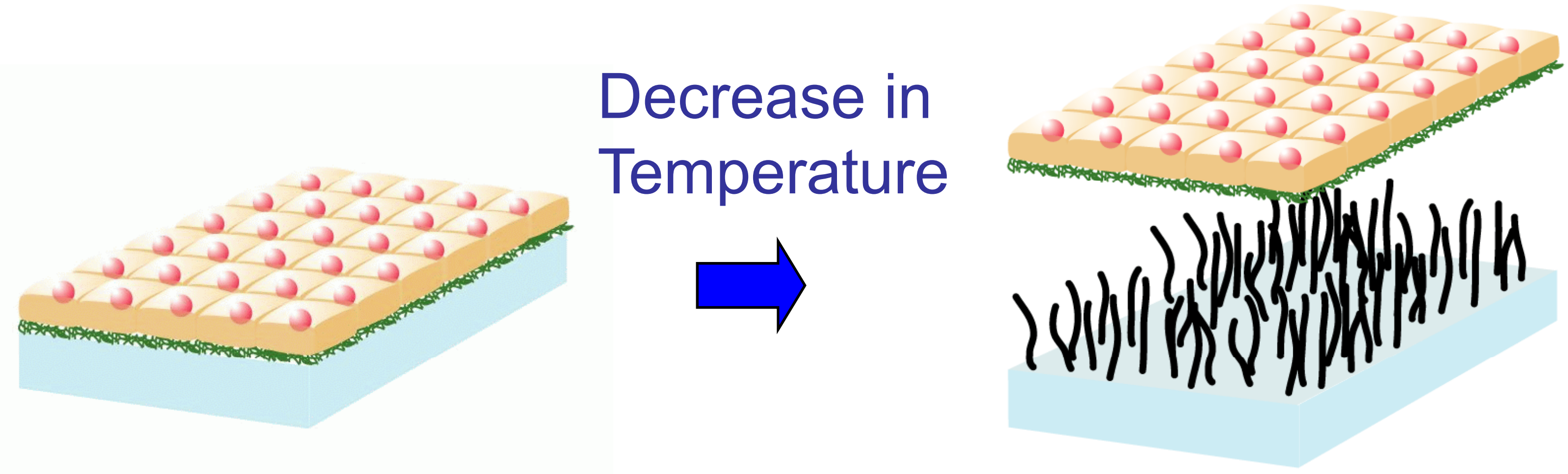

At 37°C

At 32°C below LCST

Hydrophobic surface
(Cell can attach the surface.)

Hydrophilic surface
(Cells can’t attach the surface)

Okano et al. *J. Biomed. Mater. Res.* 1993, Takezawa et al. *Biotechnology* 1990

Regenerable cell culture dish

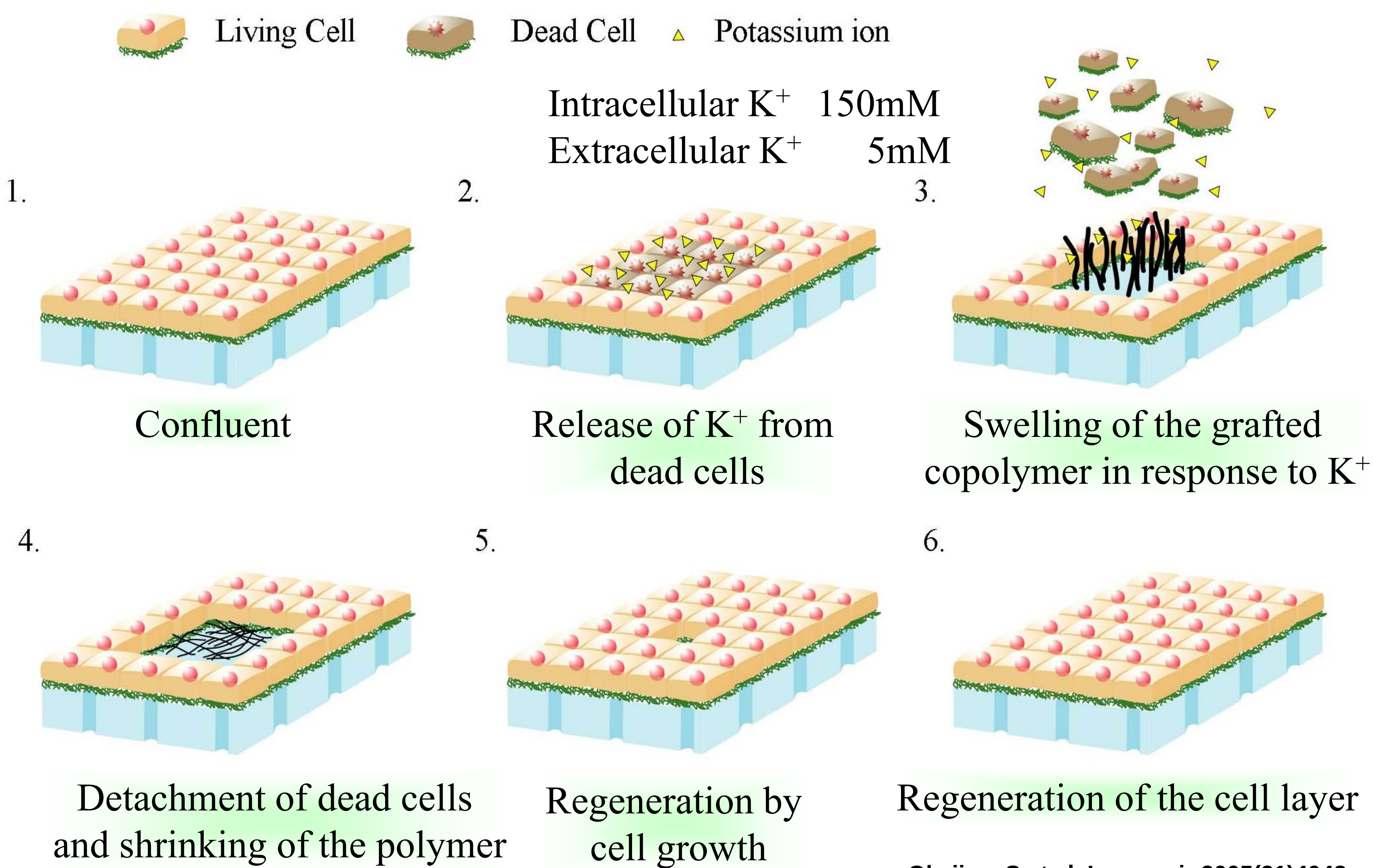

Okajima S et al. Langmuir 2005(21)4043

Detachment of dead cells

Ultraviolet light

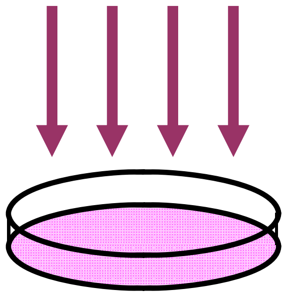

Whole irradiation for 3min

1 day

Count dead cells in culture media

trypsinization

Count attached dead cells

(using hemocytometer)

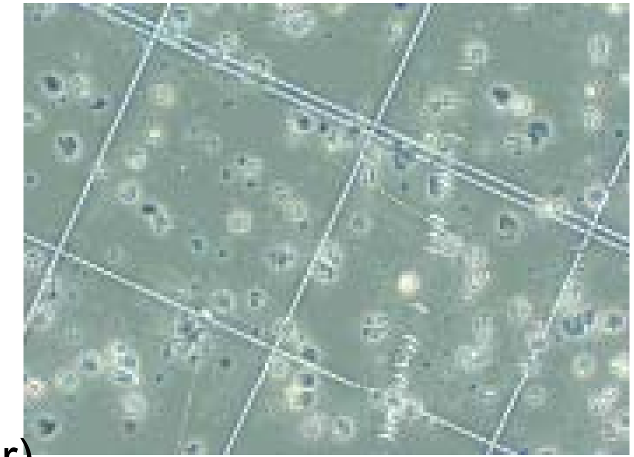

Detached dead cells

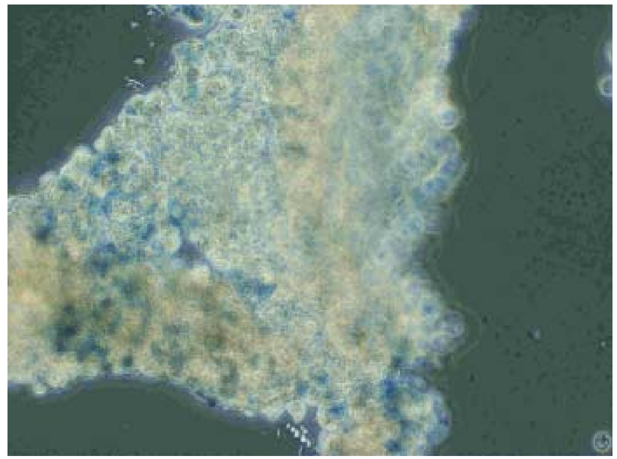

Detached living cells

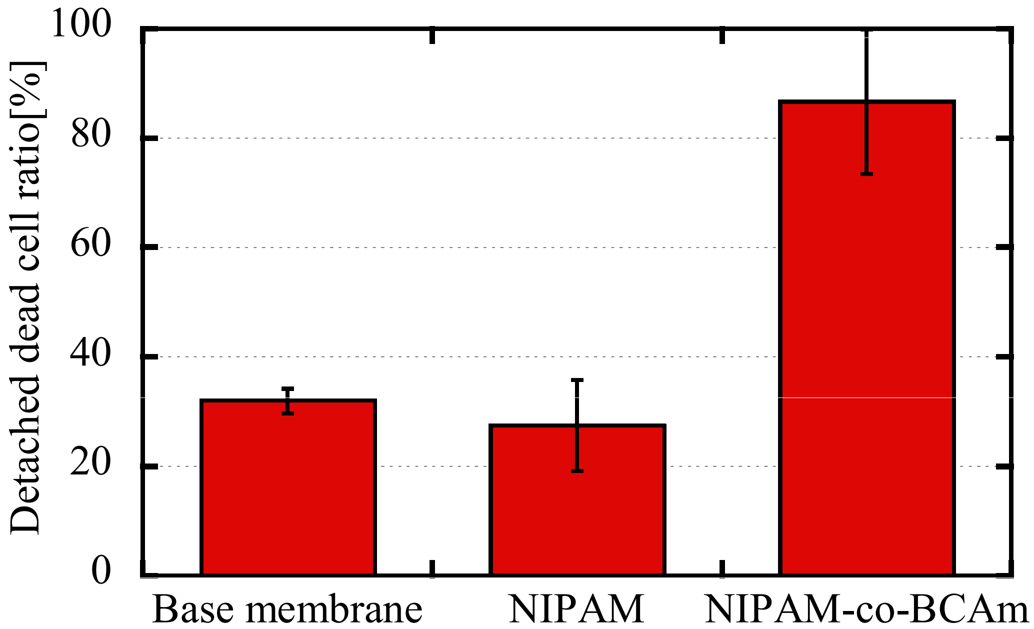

Fig. Detachment ratio of dead cells

After partial irradiation

a) PE-g-NIPAM film

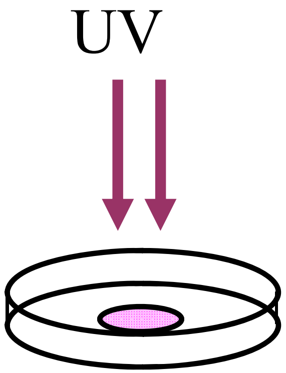

Partial irradiation
Diamter:3mm

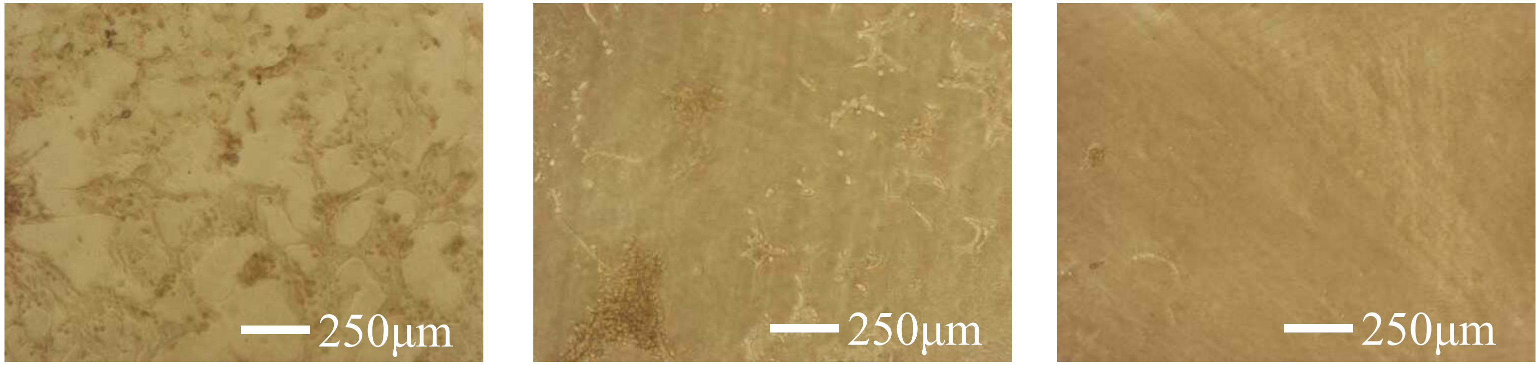

30 hours | **3 days** | **10 days**

b) NIPAM-co-BCAm

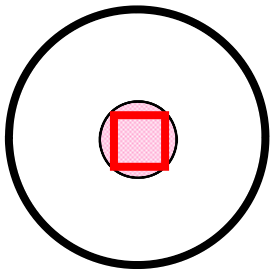

Observation Area

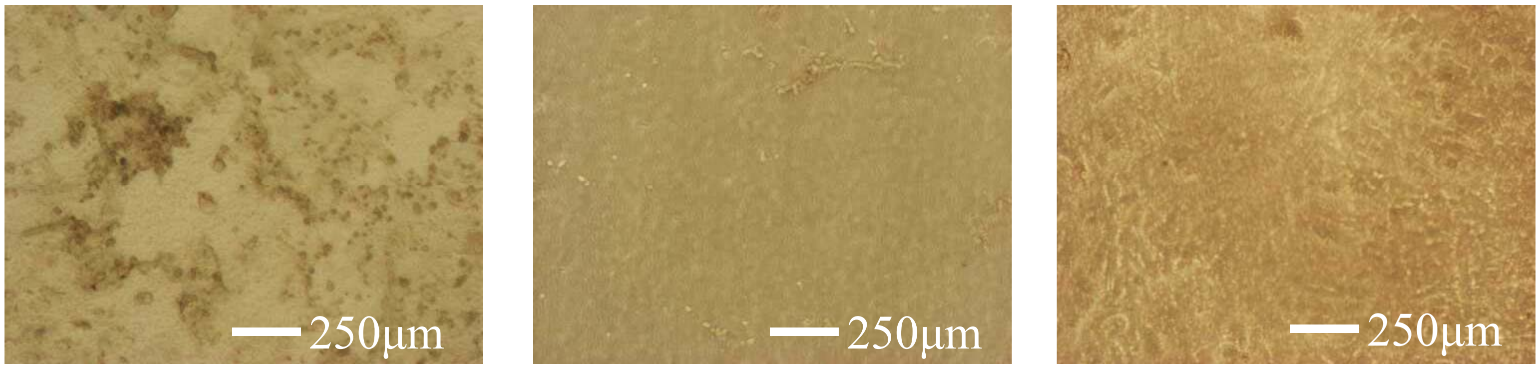

30 hours | **3 days** | **10 days**

Time course of the detachment area

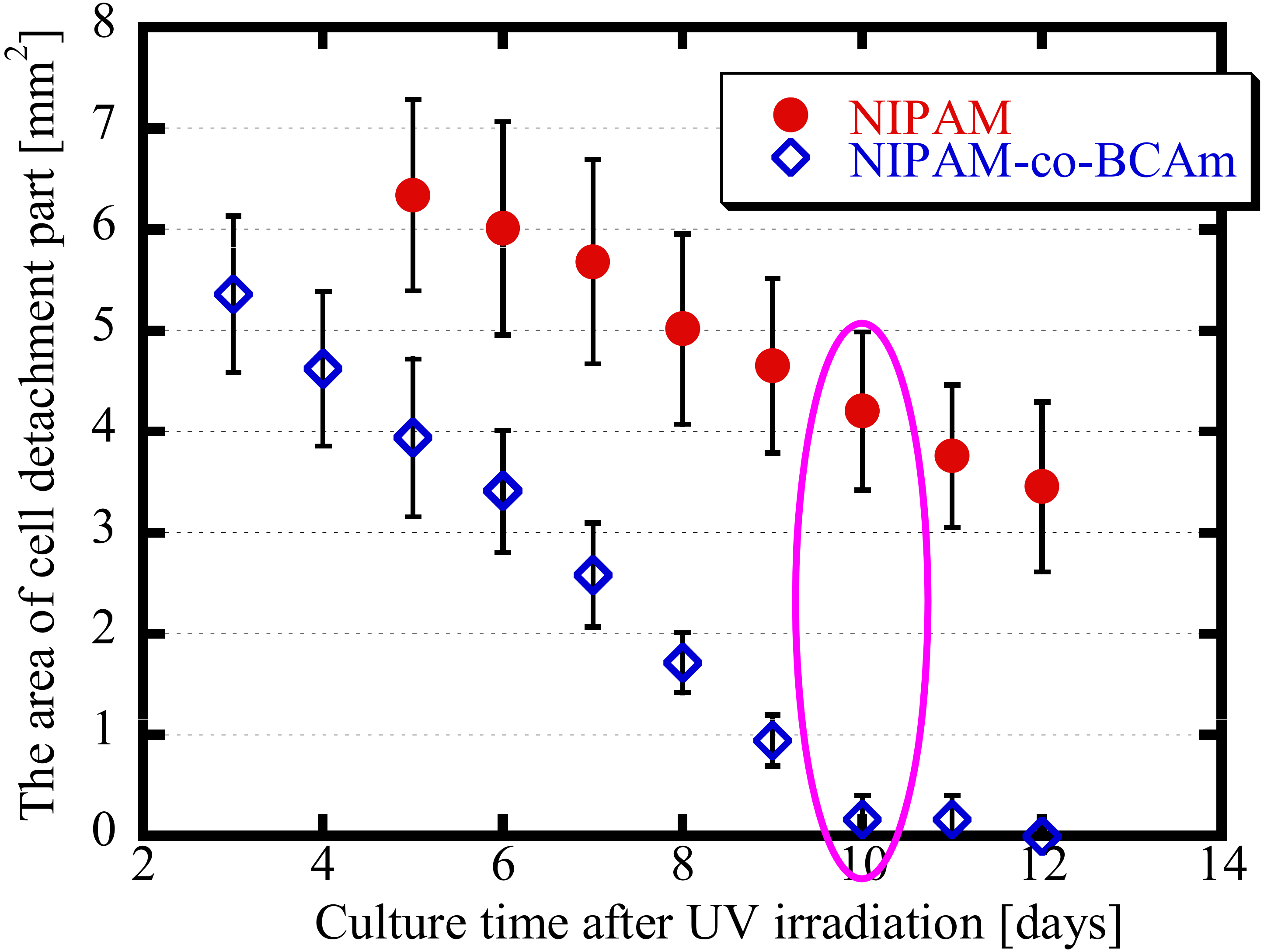

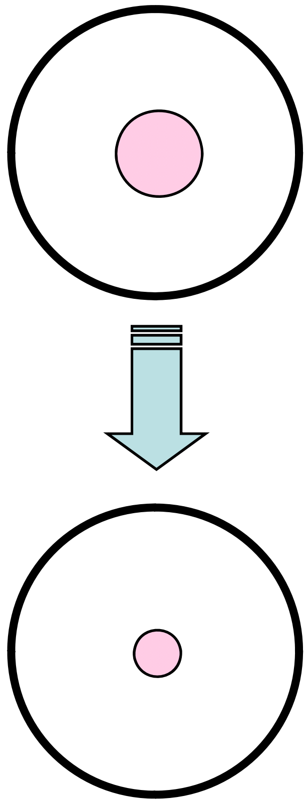

Regeneration of
a cell layer

Picture of the detachment area

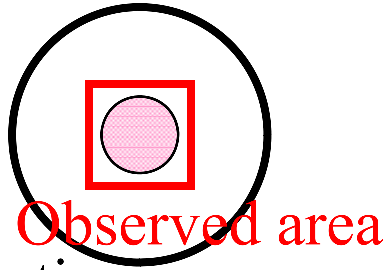

Low-magnified pictures on the 10th day after UV irradiation

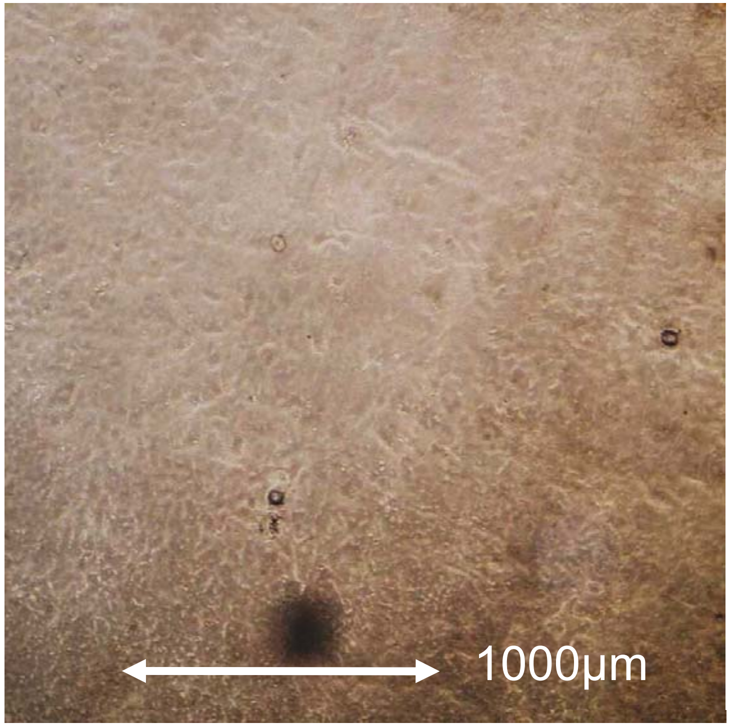

PE-g-NIPAM-co-BCAm film

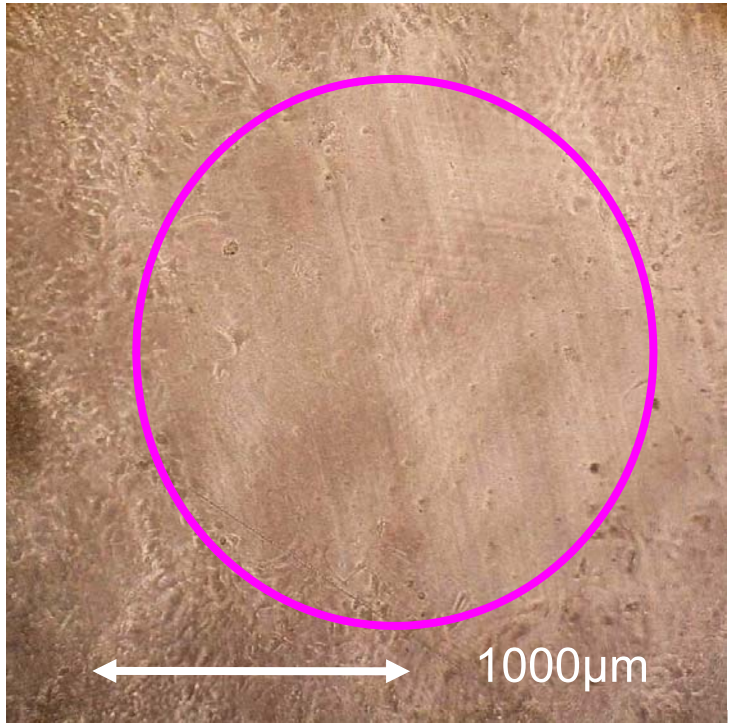

PE-g-NIPAM film

Regeneration rate increased due to the detachment of dead cells.

Inflammation

Cell death → Apotosis

Cell death → Necrosis → Inflammation

Cell derived inflammation mediators

Name	Type	Source
Histamine	*Vasoactive amine*	Mast cells, basophils, platelets
IFN-γ	Cytokine	T-cells, NK cells
IL-8	Chemokine	Primarily macrophages
Nitric oxide	*Soluble gas*	Macrophages, endothelial cells, some neurons
Prostaglandins	Eicosanoid	Mast cells
TNF-α and IL-1	Cytokine	Primarily macrophages

Time course of IL-6 level

IL-6 ⇨ Inflammation mediator

UV light

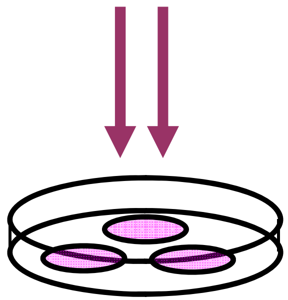

Partial irradiation
Diameter: 6mm
3 areas

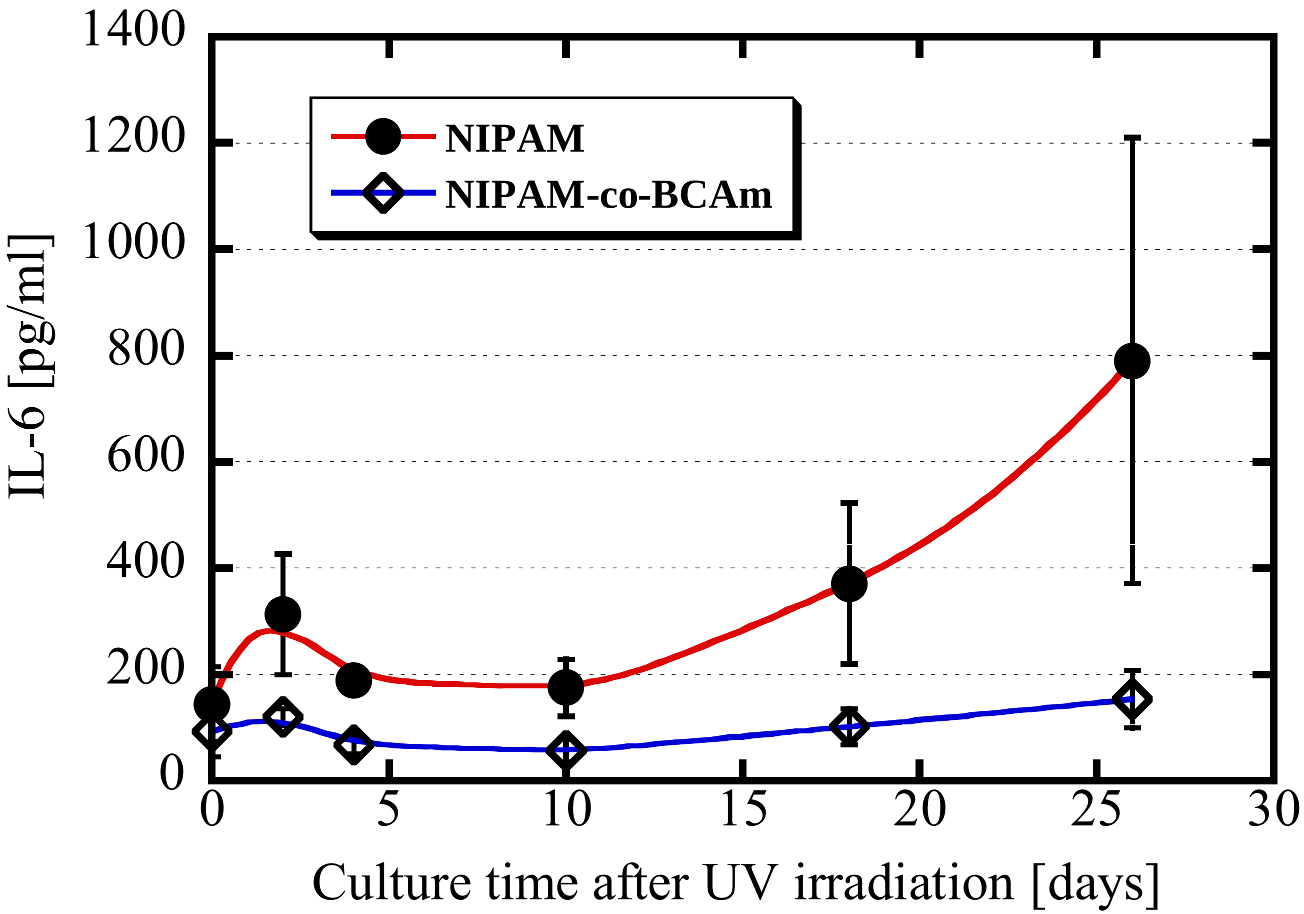

Inflammation was inhibited by the detachment of dead cells.

Artificial Energy Conversion

Fuel Cell

$$H_2 + 1/2O_2 \longrightarrow H_2O$$

$2e^-$

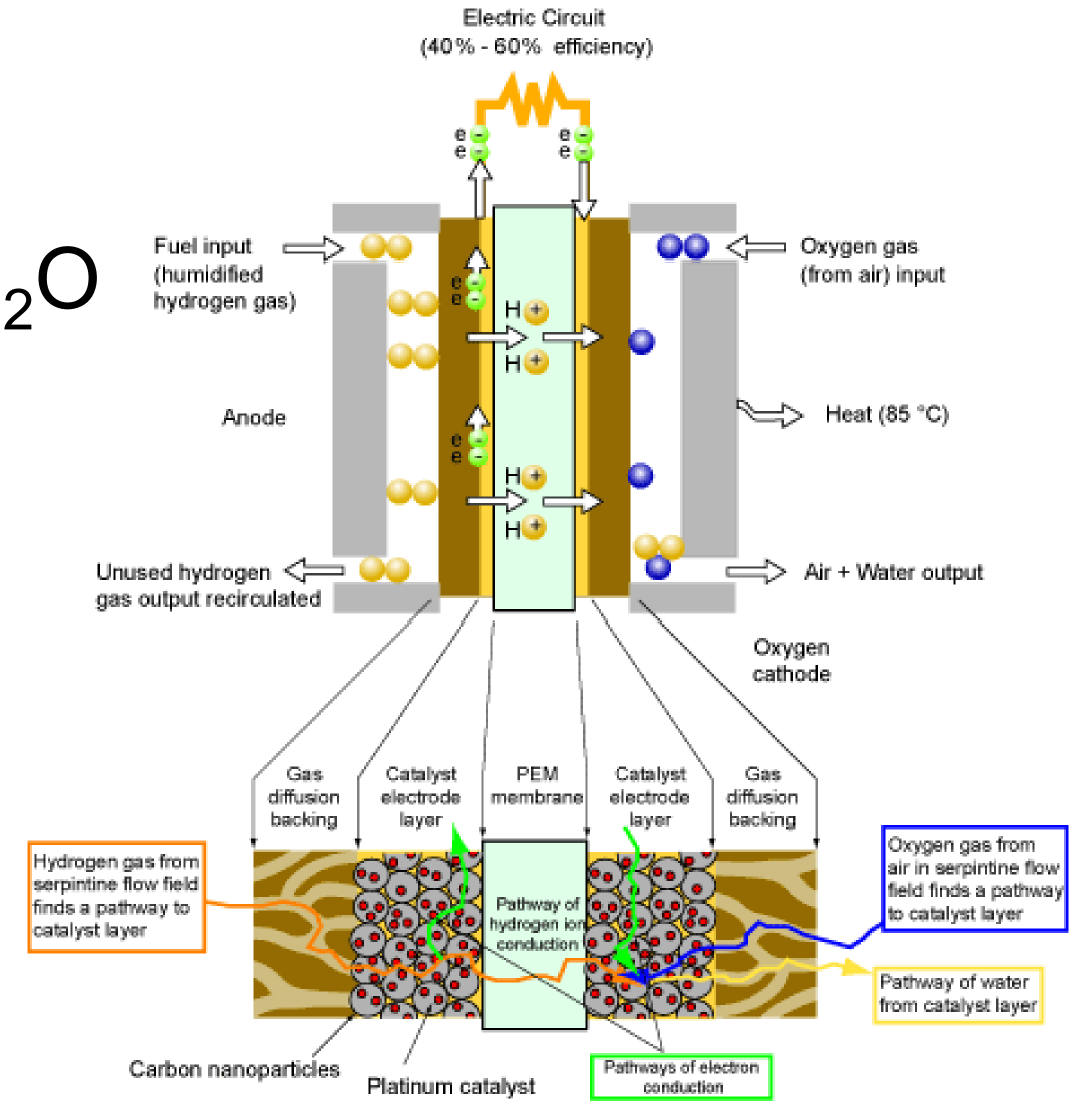

Energy metabolism of biosystem

Series of enzyme reactions

Glycolitic Pathway

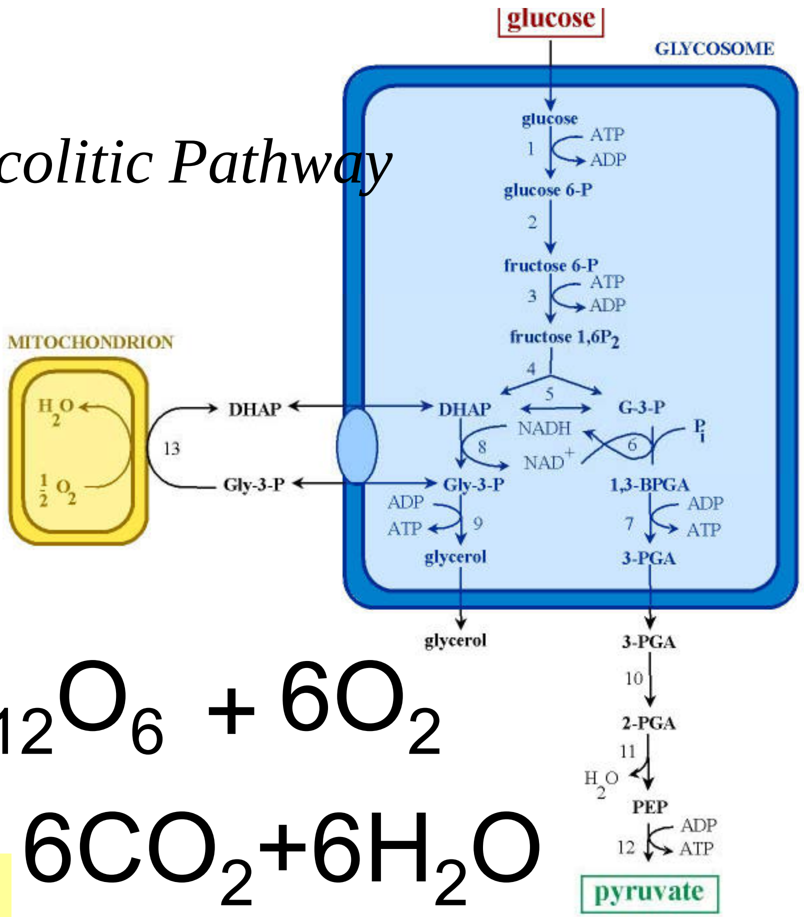

Crebs Cycle

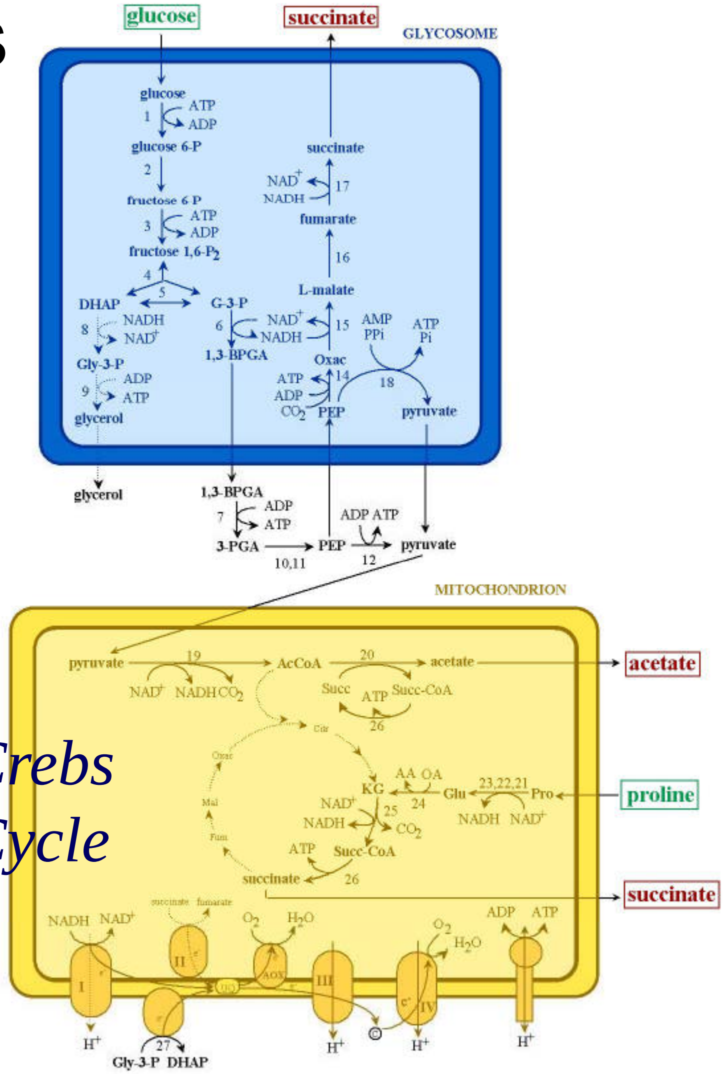

$$C_6H_{12}O_6 + 6O_2 \longrightarrow 6CO_2 + 6H_2O$$

$24e^-$

Biofuel cell

System of biofuel cell

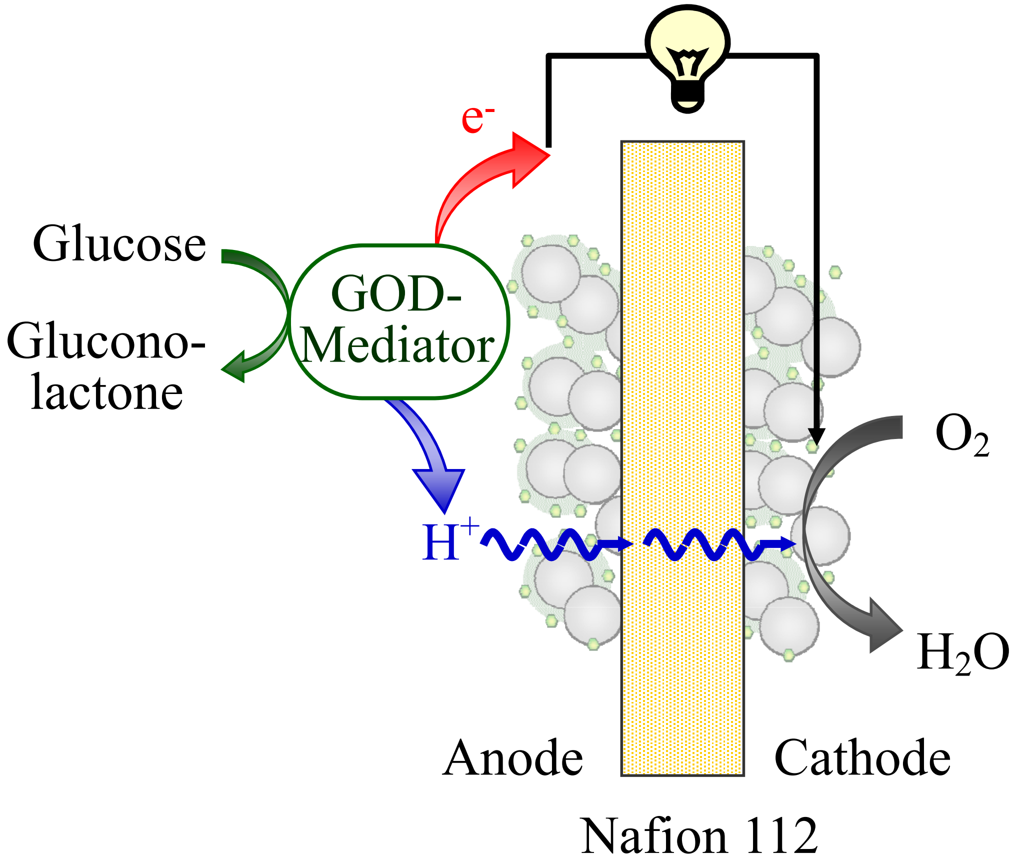

Problems of biofuel cells

Low power density

- Limited amount of enzymes effectively used on electrodes

  - Redox polymer [1)]

    → Low conductivity (∼10^{-4} S/cm)

  - Porous carbon electrodes [2), 3)]

    → Pore size: several tens of μm

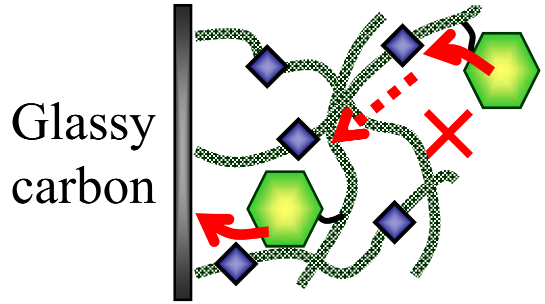

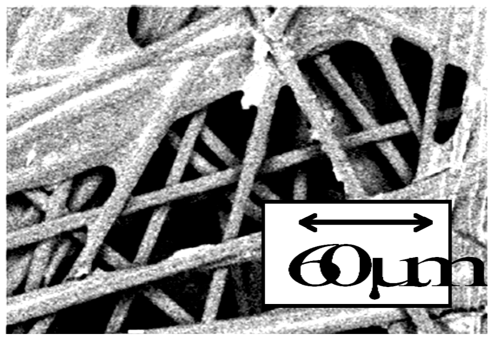

< Rate limiting factor >
Electron conduction via the redox polymer

1) N. Mano, F. Mao, *Chembiochem.*, **5**, 1703(2004),
2) S. C. Barton, *J. Phys. Chem. B*, **105**, 11917(2001)
3) S. Tsujimura et al., *Electrochem. commun.*, **5**, 138(2003)

Design of a new system

1. Increase in the Current density - Overcome the rate-limiting step

▪Dividing the electron conduction into carbon and redox polymer

Carbon: Main role in electron conduction
Redox polymer: Enzyme → Carbon

▪Increasing the real surface area

Use of carbon black (diameter ~ 30 nm)

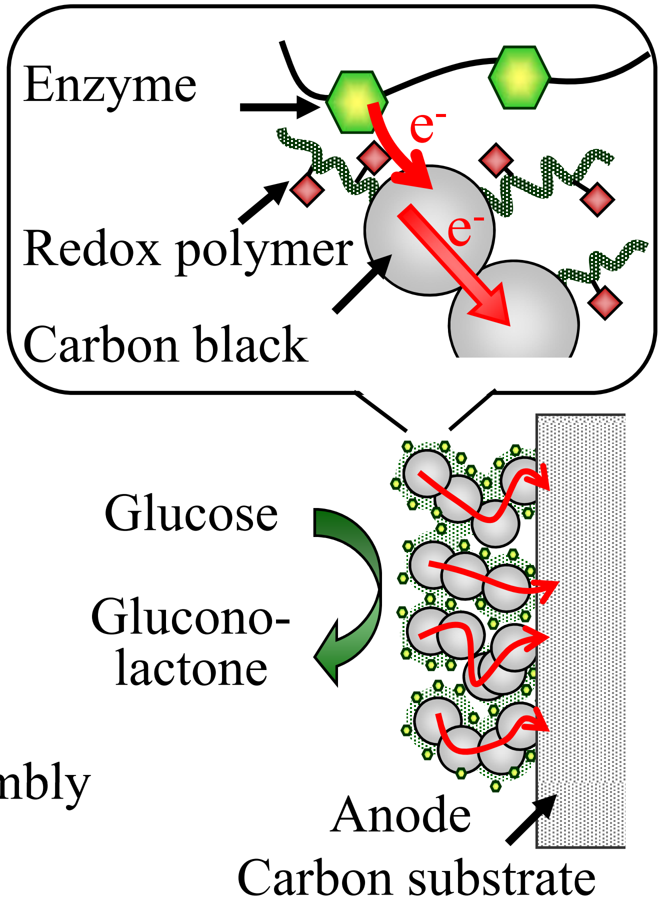

2. All solid-type biofuel cell

Membrane (polymer electrolyte) electrode assembly

3. Increase in the cell voltage

4. Model calculation to evaluate the effectiveness of electrodes

Graft Polymerization

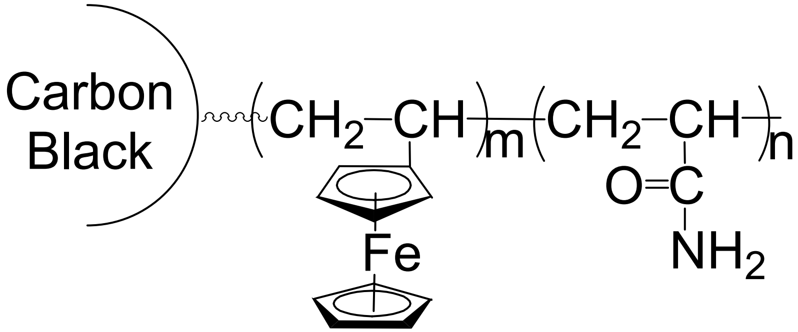

- ○Vinylferrocene(VFc)
  Mediator
- ○Acrylamide(AAm)
  Hydrophilicity

Radical graft polymerization on Carbon[1)]

Initiating groups introduced on carbon

1. Redox system consisting of -OH group and Ce^{4+}
2. Peroxyester group
3. Azo group

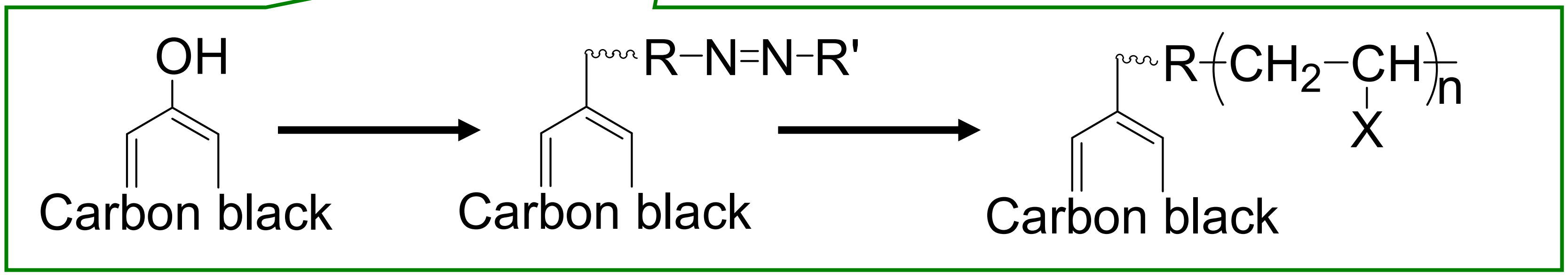

1) N. Tsubokawa, *Prog. Polym. Sci.*, **17**, 417(1992)

Electrochemical Characterization of Redox Polymer

< Cyclic Voltammetry >

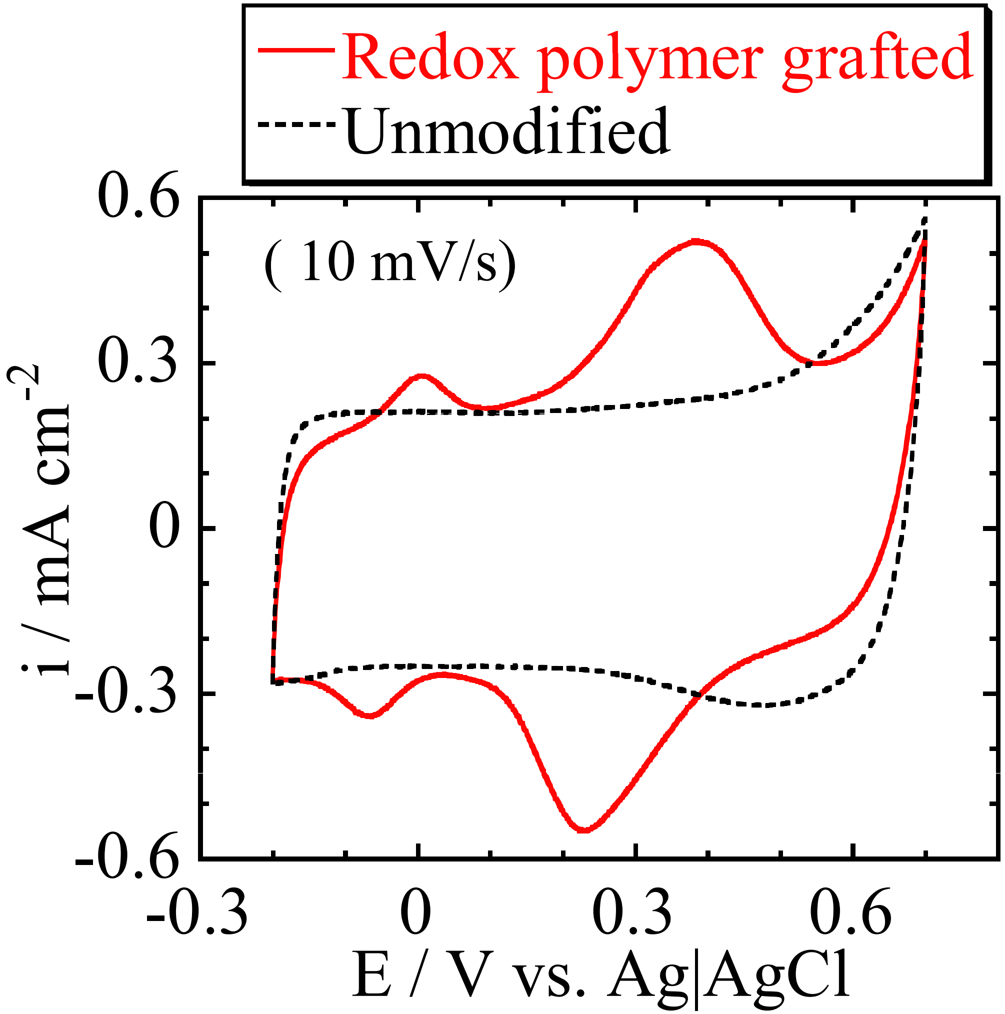

(pH 7, 0.1 M phosphate buffer)

Redox polymer grafted

Anodic and cathodic peaks

$E^{0'}$ = 0.3 V vs. Ag|AgCl

Assigned to oxidation and reduction of VFc*

Grafted redox polymer
||
Electrochemically active

*) A. E. G. Cass et al., *Anal. Chem.*, **56**, 667(1984)

T. Tamaki et al., *Ind. Eng. Chem. Res.*, **45**, 3050(2005)

Enzyme Incorporation

1-2. Immobilization of Enzymes

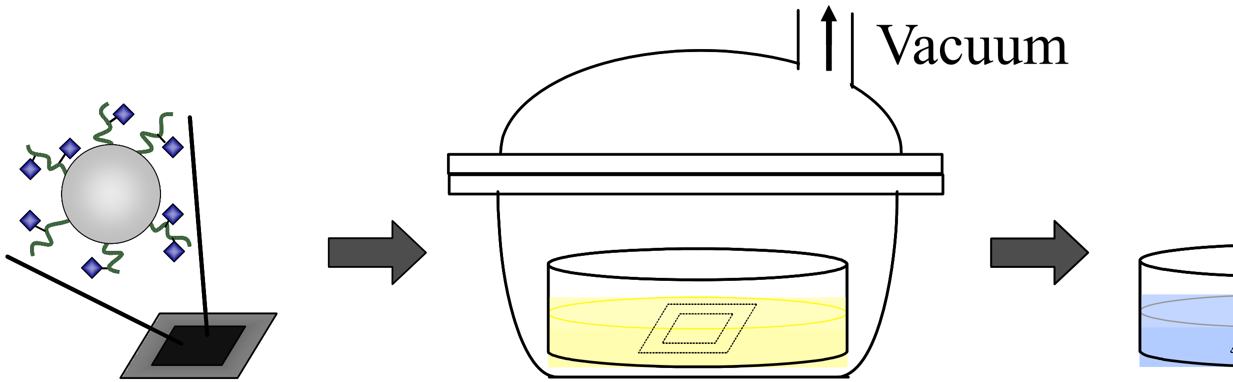

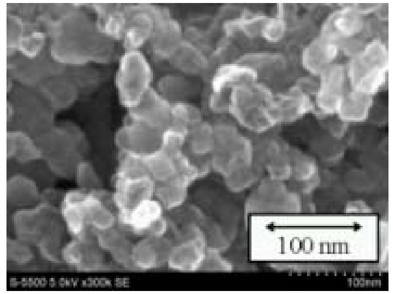

Cyclic voltammetry(CV)

- Solution: 0.1 M phosphate buffer
- Scan range: 0～0.6 V (vs Ag|AgCl)
- Scan speed: 5～50 mV/s

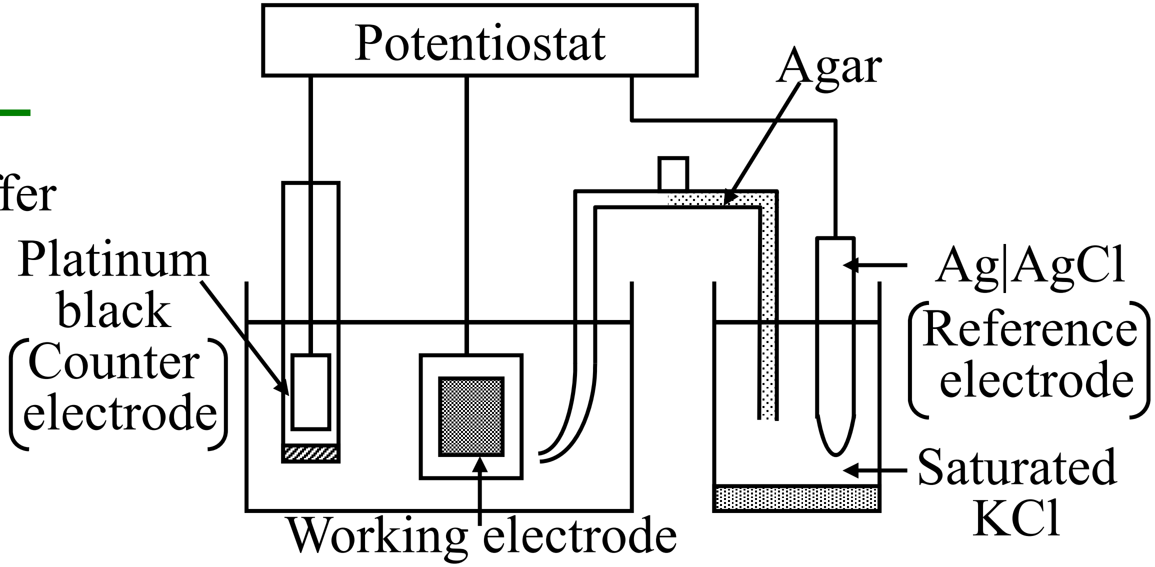

Electrochemical Characterization of GOD Electrode

< Cyclic Voltammetry >

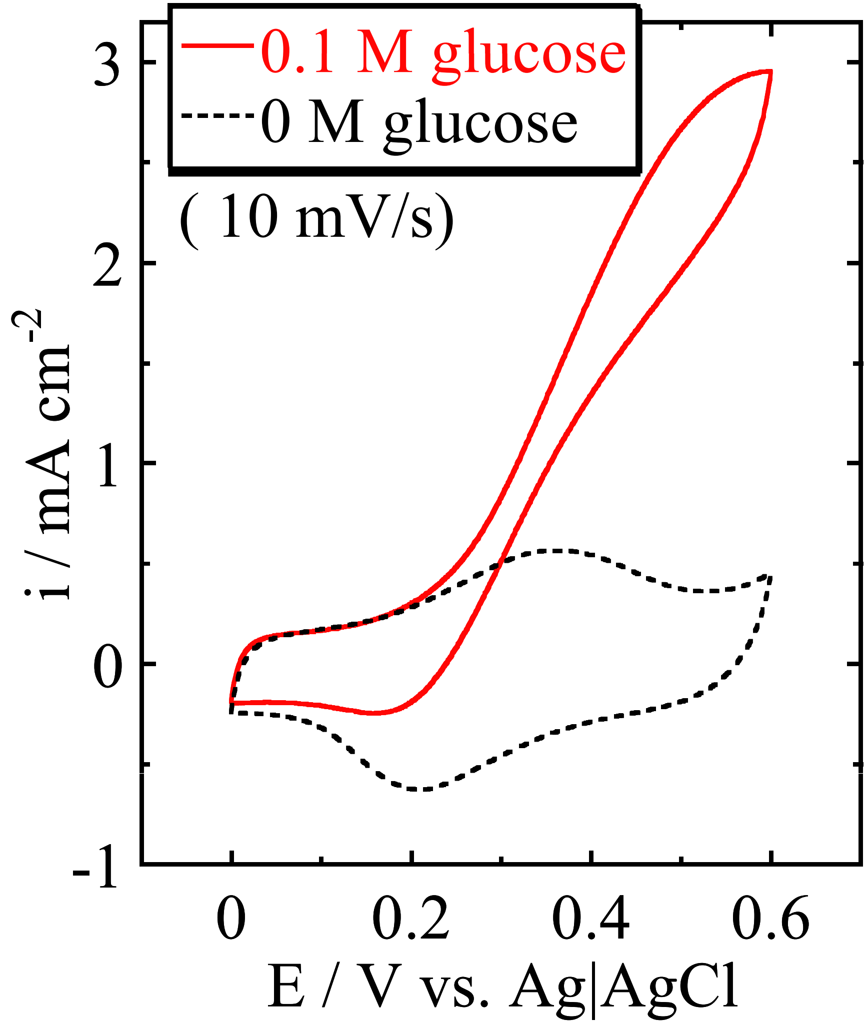

(pH 7, 0.1 M phosphate buffer)

In the presence of glucose

Enzyme catalytic reactions

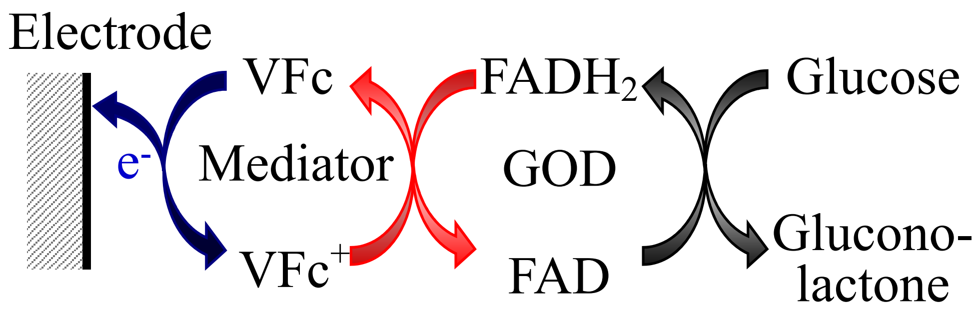

	Glucose oxidation current [mA cm^{-2}]
This study	3.0
Literature [1)]	1.5

1) N. Mao et al., *Chem. Commun.*, 2116(2004)

Further evaluated by model calculation

T. Tamaki et al., *Ind. Eng. Chem. Res.*, **45**, 3050(2005)

All-Solid Type Biofuel Cell

< Previous studies >

Electrolyte: Solution

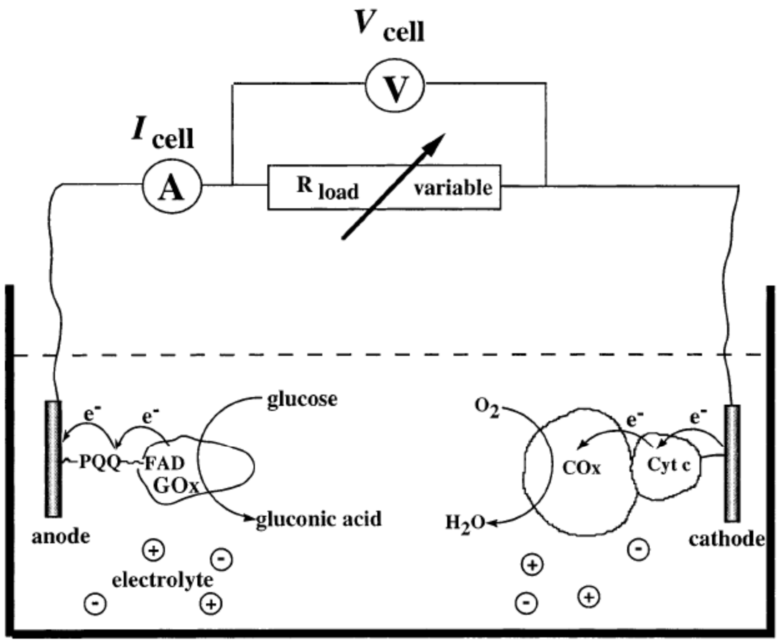

< This study >

Electrolyte: Proton conducting polymer

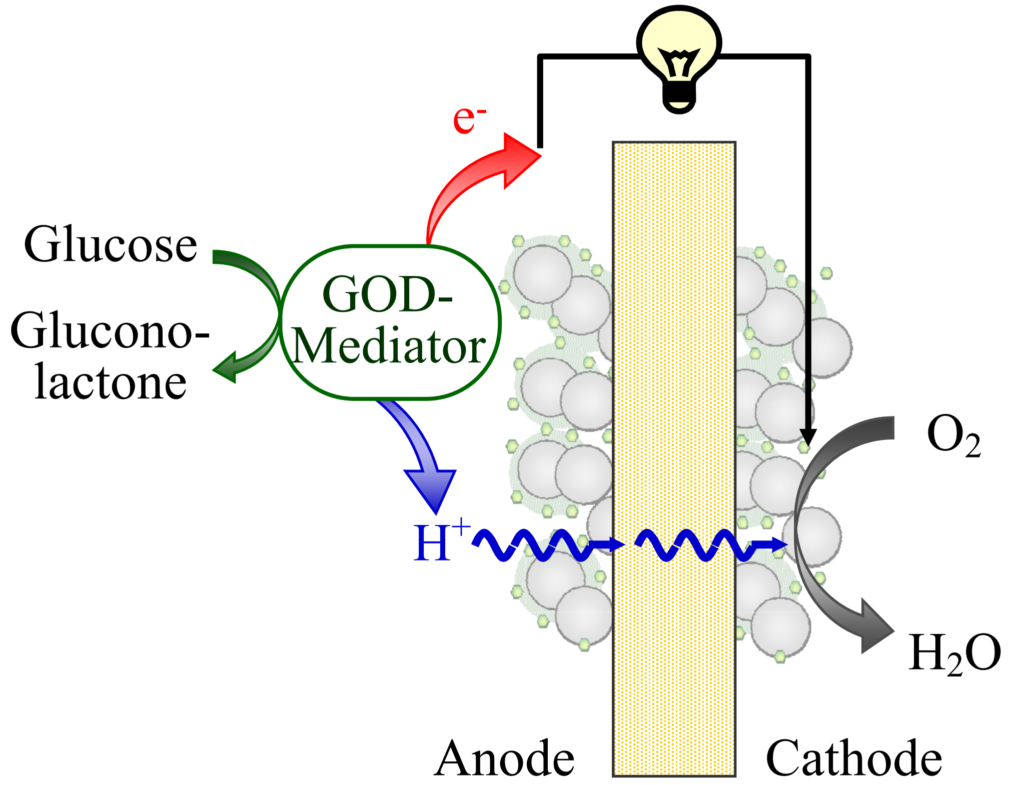

= Membrane-electrode assembly (MEA)

Fabrication of MEA Type Biofuel Cell

MEA Fabrication

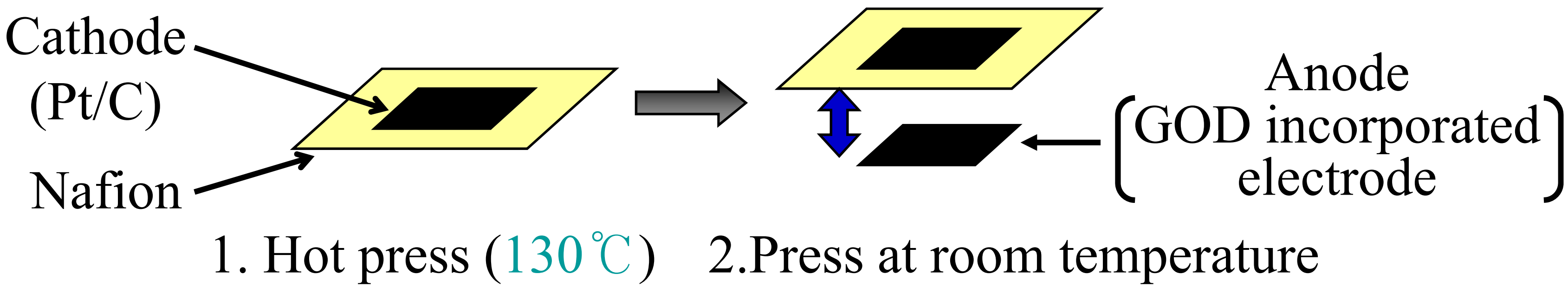

Fuel Cell Experiment

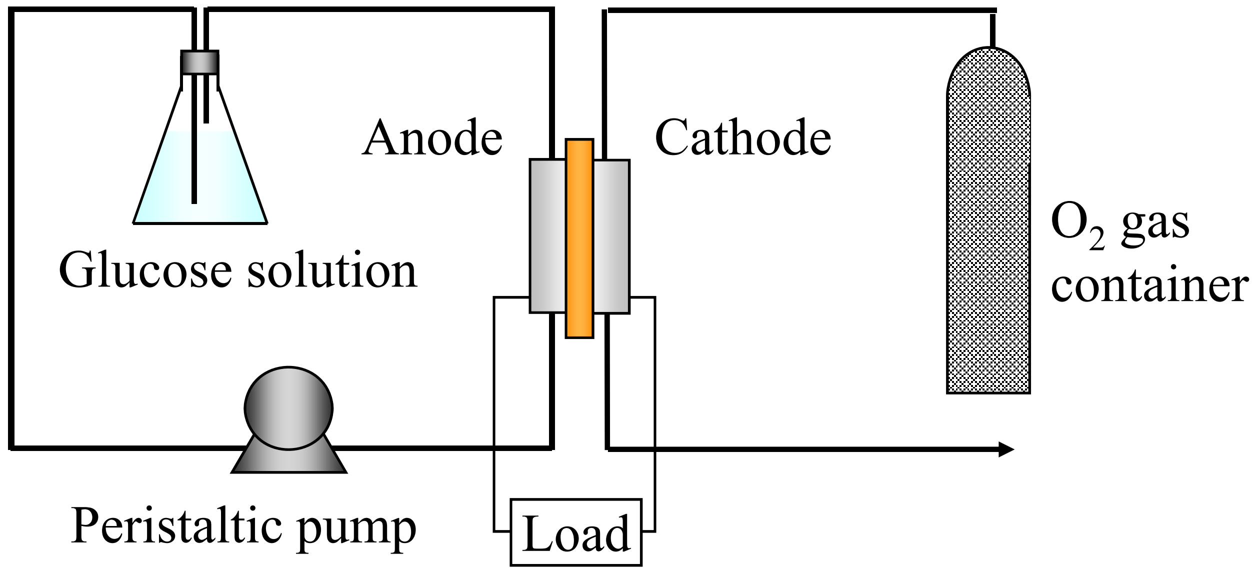

Cell Performance

- Anode: GOD-incorporated electrode
- Cathode: Pt/C (Pt = 1.0 mg/cm^2)
- Polymer electrolyte: Nafion112

Fuel: 0.1 M glucose aq.
(10 ml/min)
Oxidant: O_2 (100 ml/min)

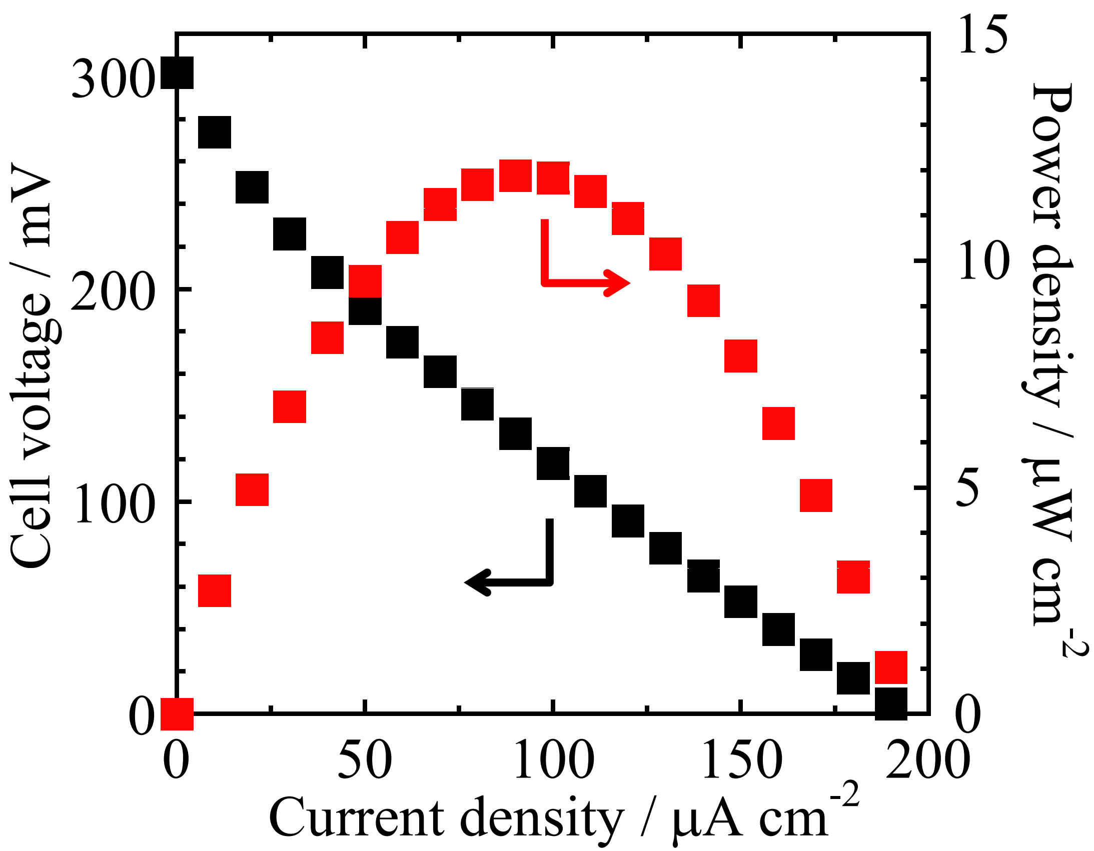

MEA style biofuel cell

Succeeded in power generation

rate limiting factor
→ proton conduction

Nernst-Einstein equation

$$\sigma = \frac{C_i z_i^2 F^2 D_i}{RT}$$

Cell Performance after Incorporation of Nafion

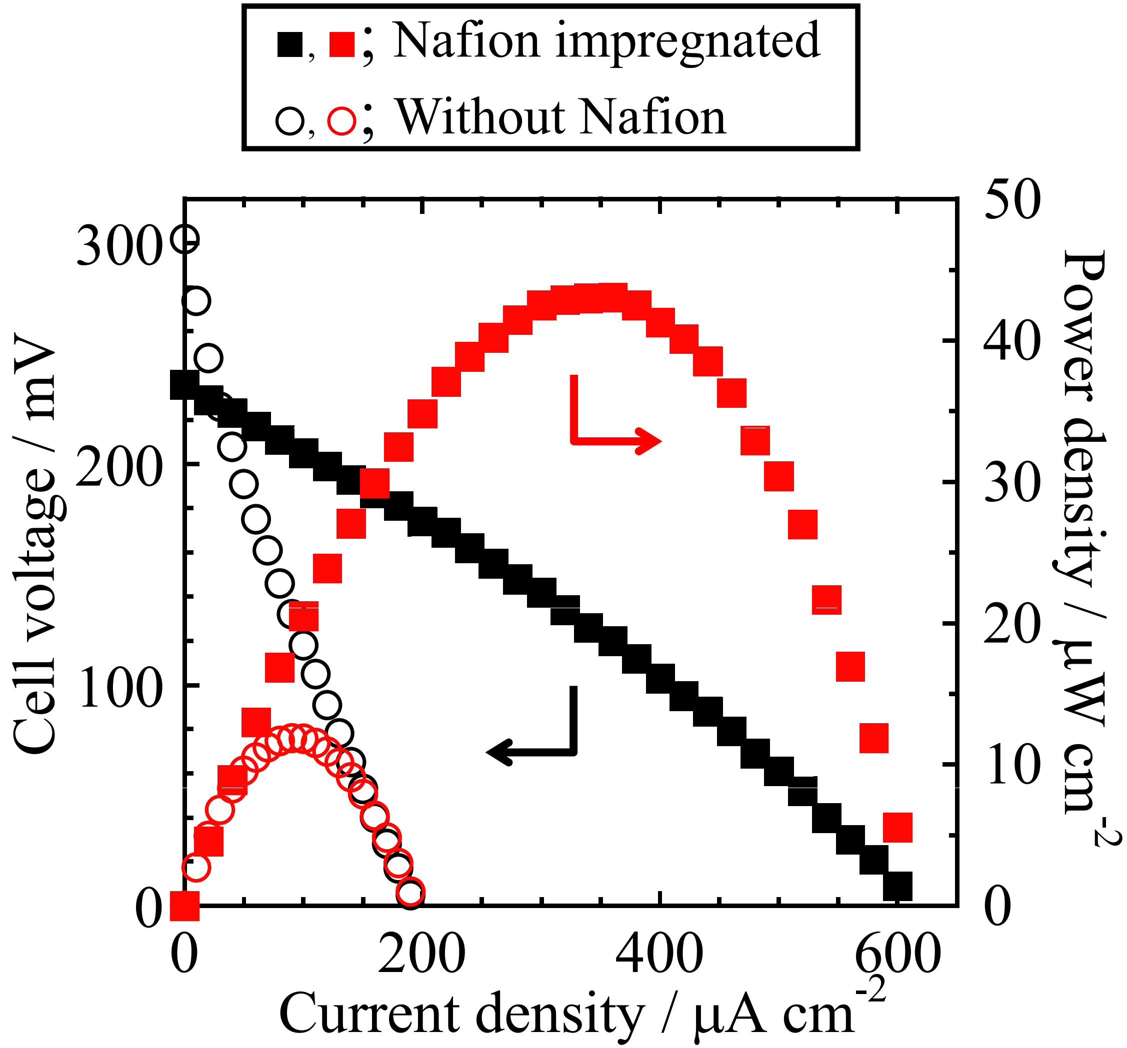

Increases in
cell performances

Improvement in
proton conduction

Deactivation of GOD
(local decrease in pH)

Use of other proton
conducting polymers
(with high pKa)

T. Tamaki et al., *Ind. Eng. Chem. Res.*, **45**, 3050(2005)

Effect of Proton Conducting Polymer on GOD Activity

GOD activity: Measured by O_2 consumption rate

ATBS:

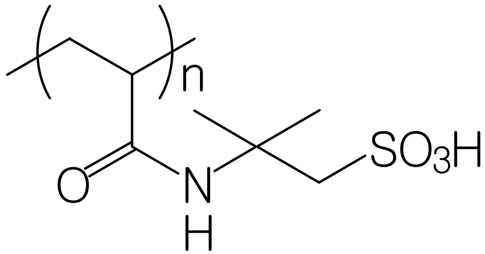

PVP:

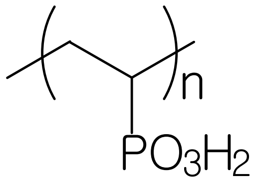

PAAc:

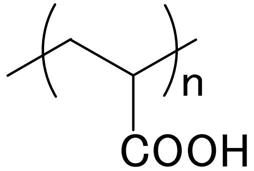

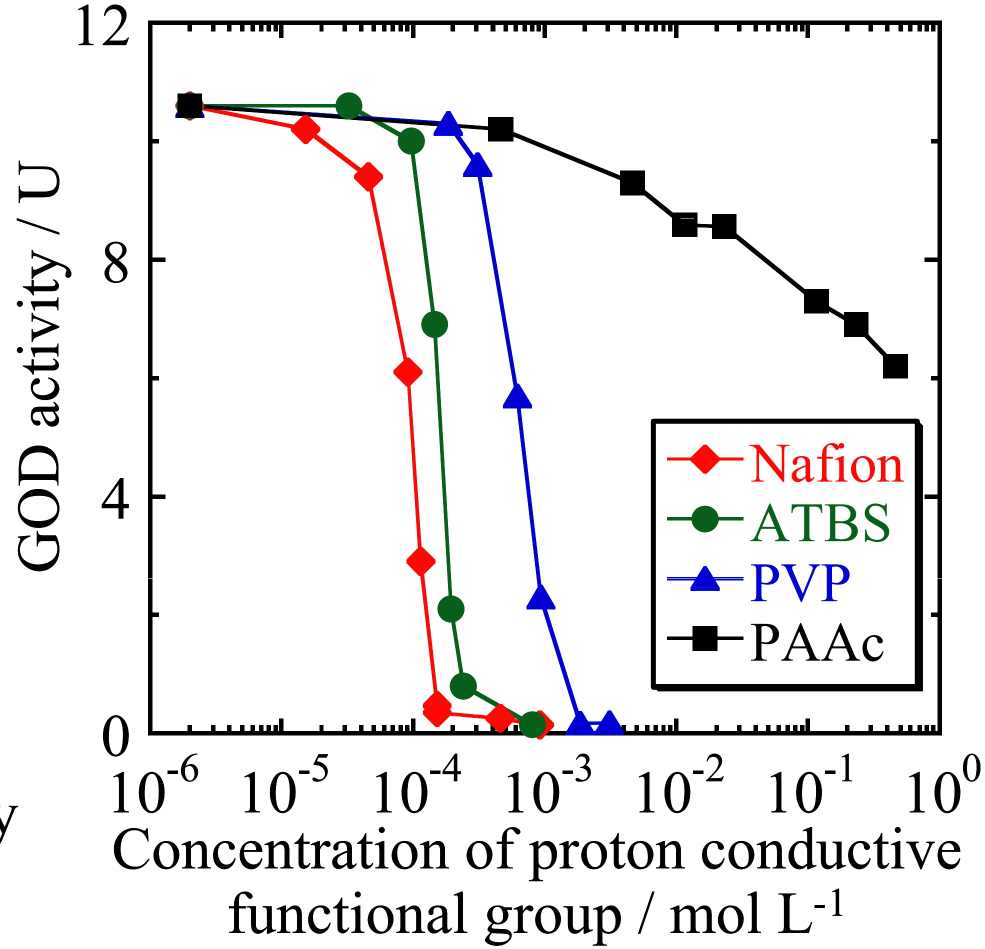

pKa → Effect on GOD activity

↕

pKa → Proton conductivity

< Need optimization of material and electrode structure>

Increase in the Cell Voltage

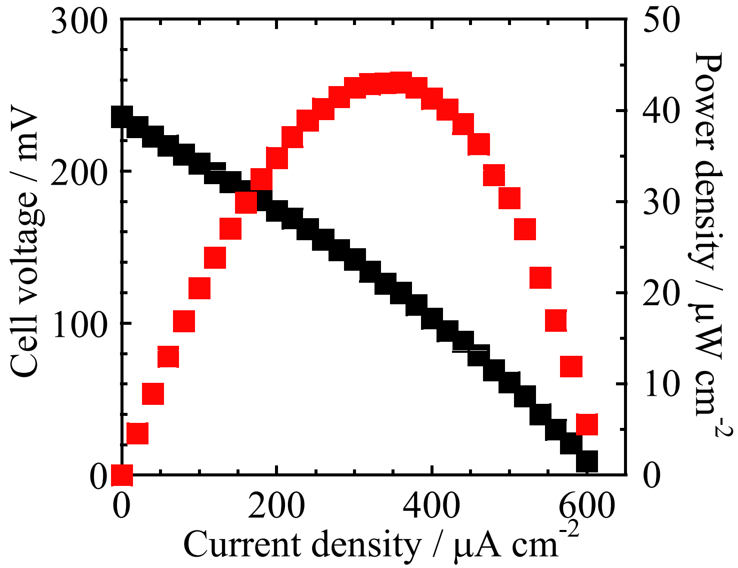

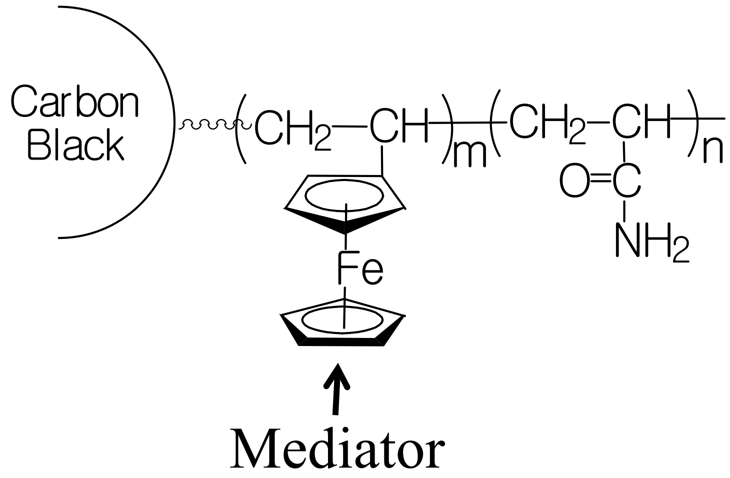

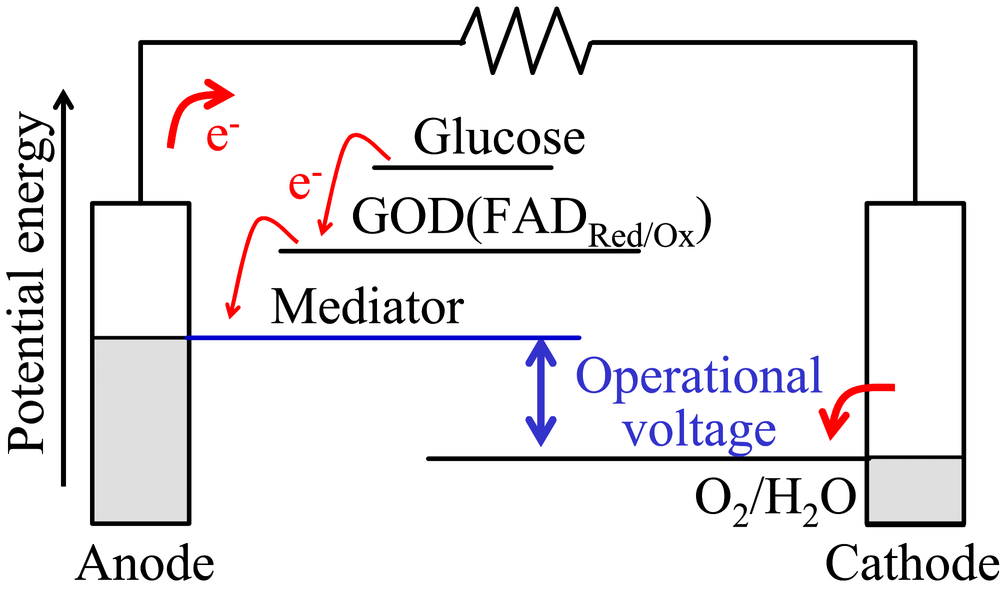

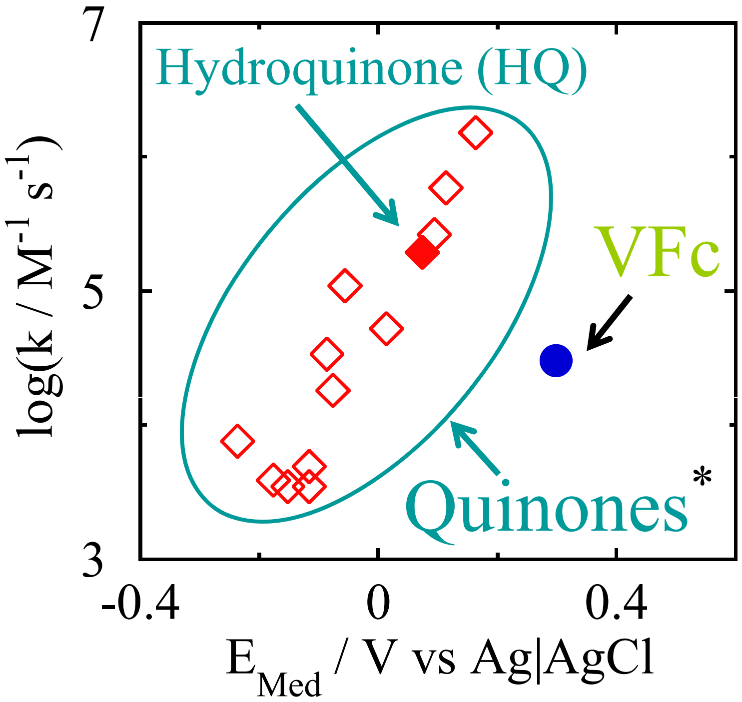

* J. Y. Kulys et al., *Biochim. Biophys. Acta.*, **744**, 57(1983), T. Ikeda et al., *Agric. Biol. Chem.*, **48**, 1969(1984)

Immobilization of HQ

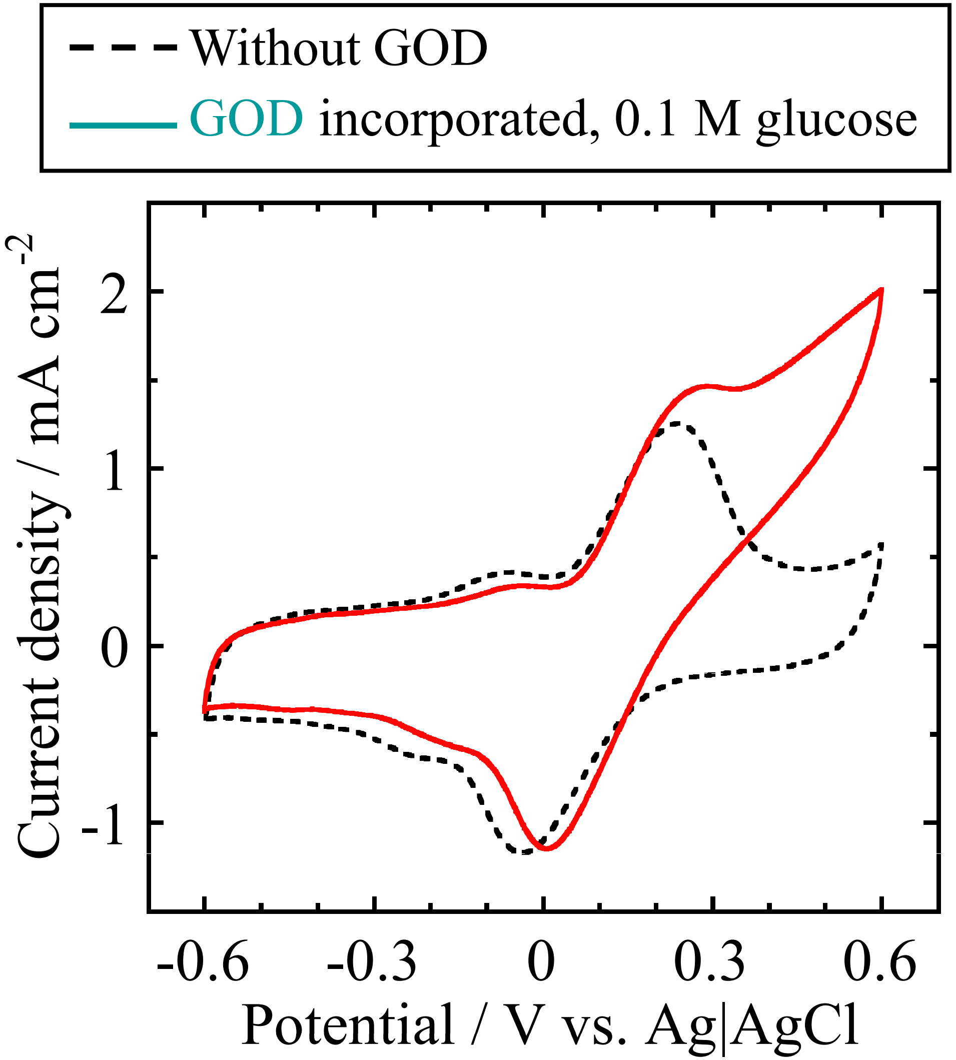

(0.1 M phosphate buffer, pH7.0)

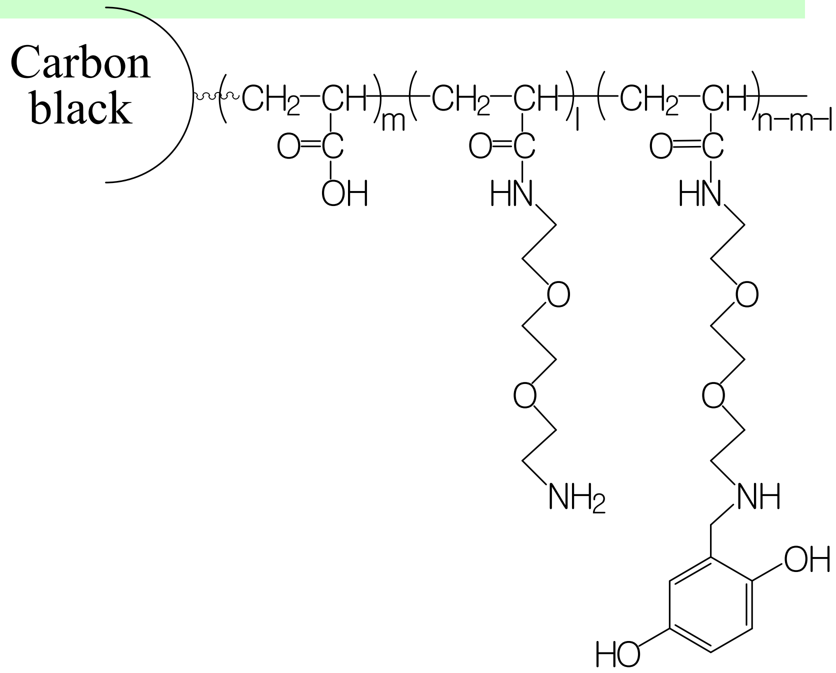

After immobilzation of HQ

Redox peaks due to HQ was obtained

GOD incorporated

Electrocatalytic cycle between GOD and HQ observed

T. Tamaki et al., *J. Phys. Chem. B*, **111**, 10312(2007)

Comparison of HQ and VFc

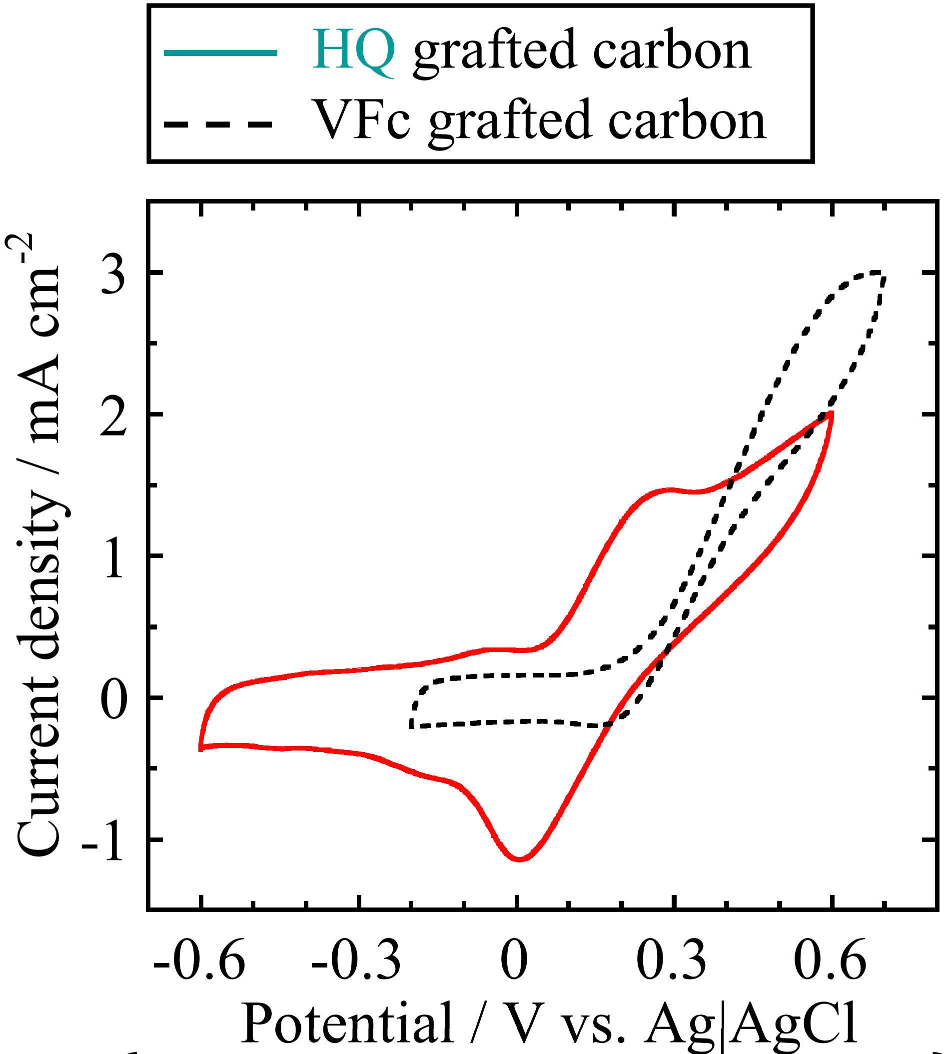

(0.1 M glucose in
0.1 M phosphate buffer, pH7.0)

- ## Current density

Increase in the same order

Regardless of mediators,
the electrode is effective

- ## Potential

Negative shift in about 0.2 V

||

Correspond to the increase in cell voltage by about 0.2 V

Model Calculation

- To Evaluate the Effectiveness of Electrodes

< Previous Research>

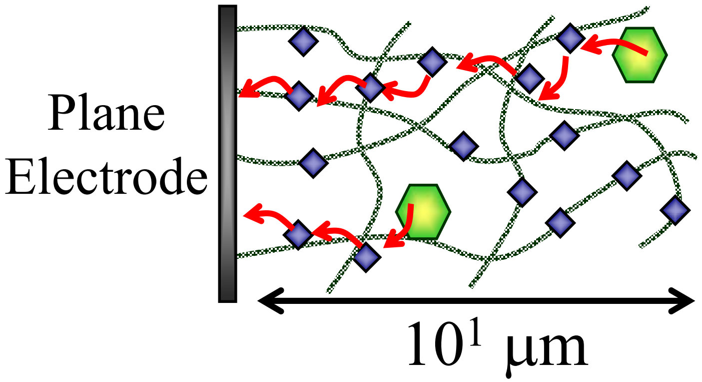

< This Study>

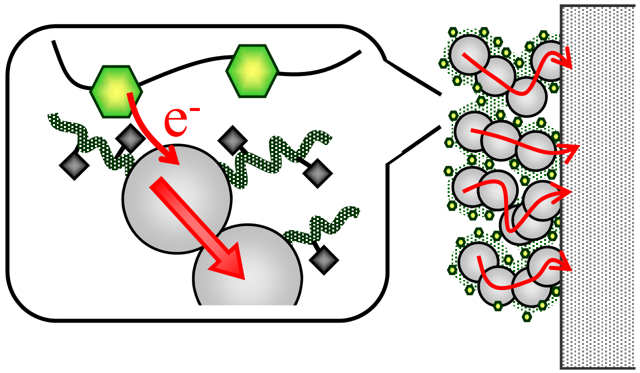

Reaction and diffusion processes to be considered

① Diffusion of substrate
② Enzyme reaction
③ Electron conduction through redox polymer

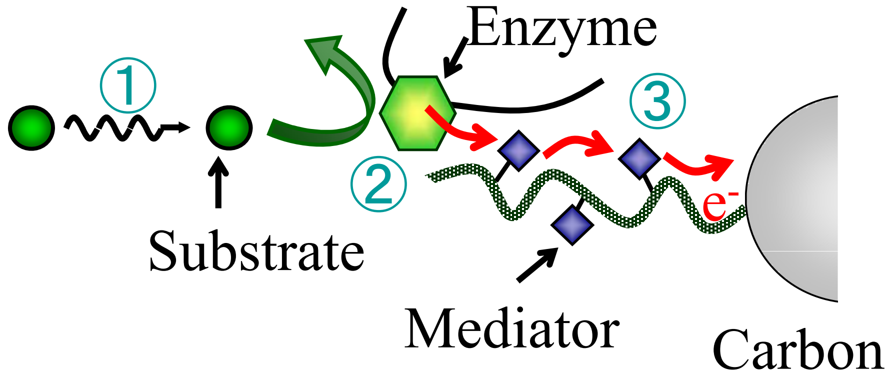

Assumptions in Modeling

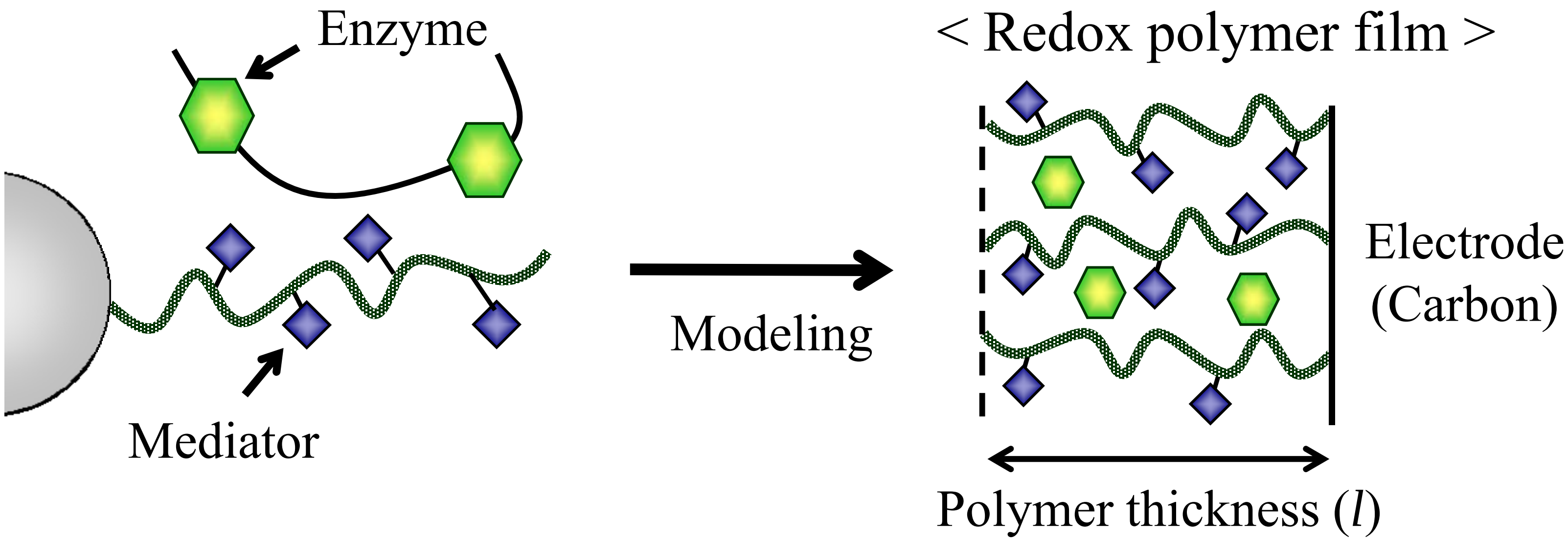

< Assumption >

- Concentration of Mediator (C_{MT}) and Enzyme (C_{ET}) : Constant at x = 0～l
- Electron conduction through redox polymer:
  - Expressed by apparent electron diffusion coefficient (D_M) in redox polymer
- Mass transport of glucose outside of the polymer film
- Proton conduction

Not considered

Enzyme Reaction

< Glucose oxidase >

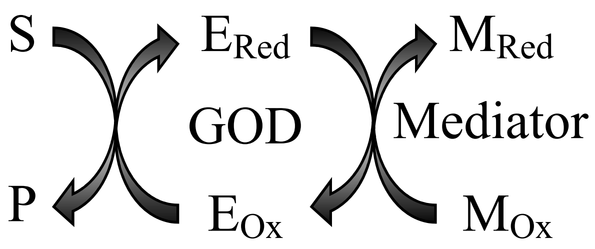

$$\begin{cases} S + E_{Ox} \underset{k_{-1}}{\overset{k_1}{\rightleftarrows}} ES \xrightarrow{k_2} P + E_{Red} & (1) \\ M_{Ox} + E_{Red} \xrightarrow{k_{med}} M_{Red} + E_{Ox} & (2) \end{cases}$$

Steady-state conditions: ES, E_{Red} (or E_{Ox})

$$v_{Enz} = \frac{k_{cat} C_{Enz}}{1 + Ks / C_S + K_M / C_{MO}}$$

$$\left(k_{cat} = k_2 \quad , \quad K_S = \frac{k_{-1} + k_2}{k_1} \quad , \quad K_M = \frac{k_2}{k_{med}} \right)$$

k_{cat}, K_S : Dependent only on eq (1)

k_{med}: Second-order rate constant between GOD and mediator

T. Tamaki et al., *Fuel Cells*, accepted

Reaction-diffusion equations

Reaction-diffusion equation

$$\begin{cases} \dfrac{\partial C_{MR}}{\partial t} = D_M \dfrac{\partial^2 C_{MR}}{\partial x^2} + 2\dfrac{k_{cat} C_{ET}}{K_s / C_s + K_M / C_{MO} + 1} & \text{(Reduced form of Mediator)} \\ C_{MO} = C_T(const) - C_{MR} & \text{(Oxidized form of Mediator)} \\ \dfrac{\partial C_S}{\partial t} = D_S \dfrac{\partial^2 C_S}{\partial x^2} - \dfrac{k_{cat} C_{ET}}{K_s / C_s + K_M / C_{MO} + 1} & \text{(Substrate = Glucose)} \end{cases}$$

Boundary condition 1: $x = 0$

$$\begin{cases} C_{MR} = \dfrac{C_T}{1 + \exp\left\{\dfrac{nF}{FT}\left(E - E^0{}_{med}\right)\right\}} \\ C_{MO} = C_T - C_{MR} \\ \left.\dfrac{\partial C_S}{\partial x}\right|_{x=0} = 0 \end{cases}$$

Boundary condition2: $x = l$

$$\begin{cases} \left.\dfrac{\partial C_{MR}}{\partial x}\right|_{x=l} = 0 \\ \left.\dfrac{\partial C_{MO}}{\partial x}\right|_{x=l} = 0 \\ C_S = C_{Sb} \end{cases}$$

Initial condition ($t = 0$, $x \geq 0$)

$$\begin{cases} C_{MR} = C_T \\ C_{MO} = 0 \\ C_S = C_{Sb} \end{cases}$$

T. Tamaki et al., *Fuel Cells*, accepted

Results of Calculation (Example)

Concentration profile (at steady state)

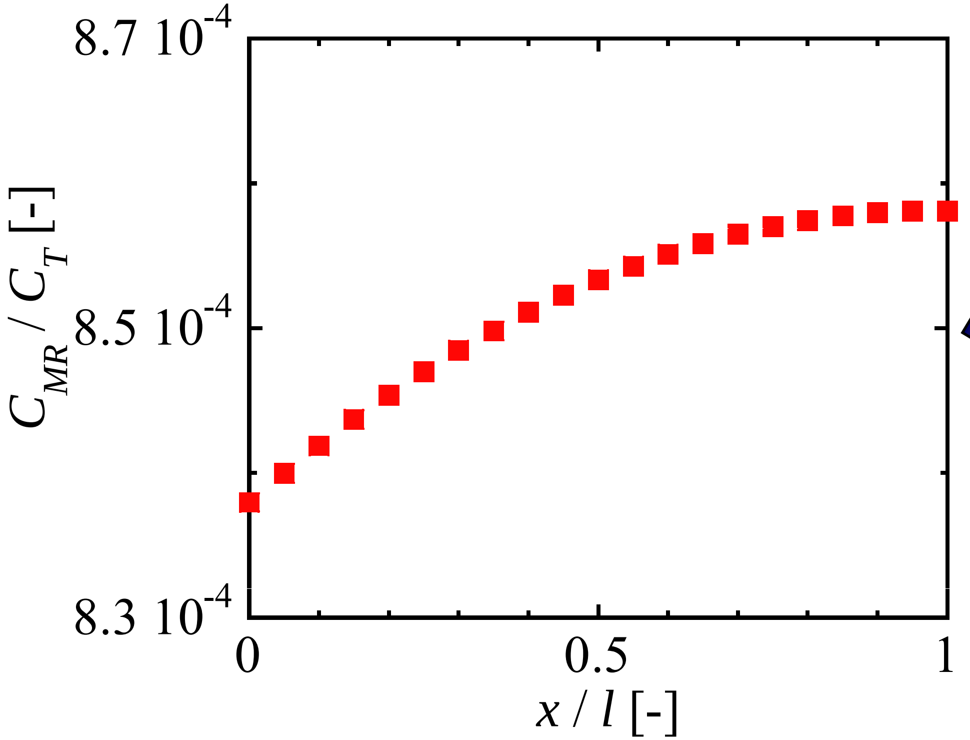

$$\left(\begin{array}{l} l = 20\ \text{nm},\ D_M = 3 \times 10^{-8}\ \text{cm}^2/\text{s} \\ Q_T = 4.8 \times 10^{-8}\ \text{mol/cm}^2 \\ Q_{ET} = 4.2 \times 10^{-11}\ \text{mol/cm}^2 \\ E = 0.48\ \text{V},\ E^0_{med} = 0.298\ \text{V} \\ A_{r\_p} = 2300 \end{array} \right)$$

$$I = nFAD_M \left. \frac{\partial C_{MR}}{\partial x} \right|_{x=0}$$

Current-Potential curve

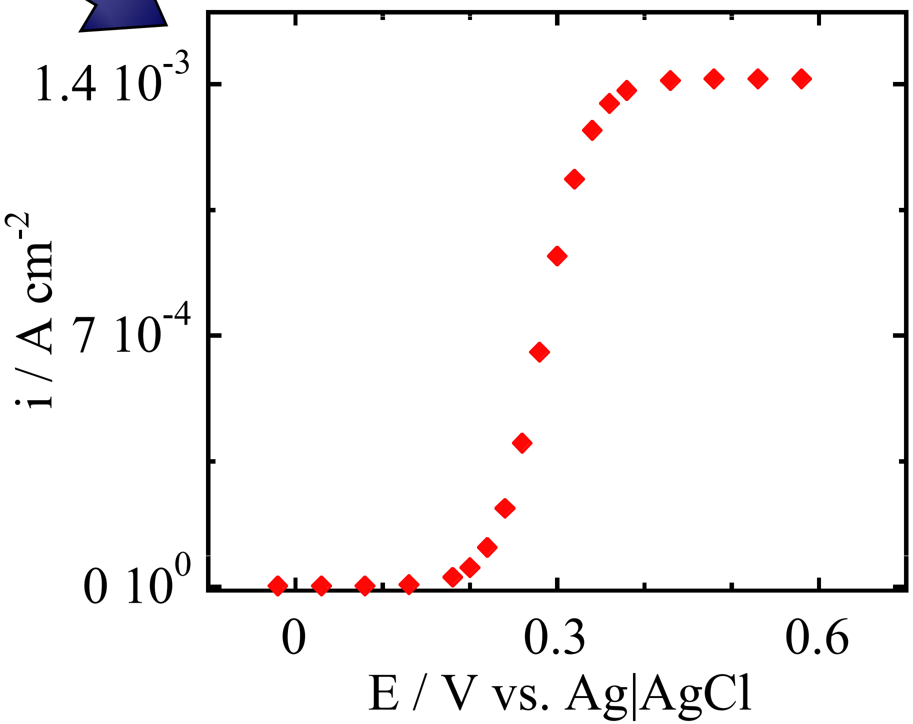

Rate Limiting Step in Previous Study

Effect of electron (apparent) diffusion

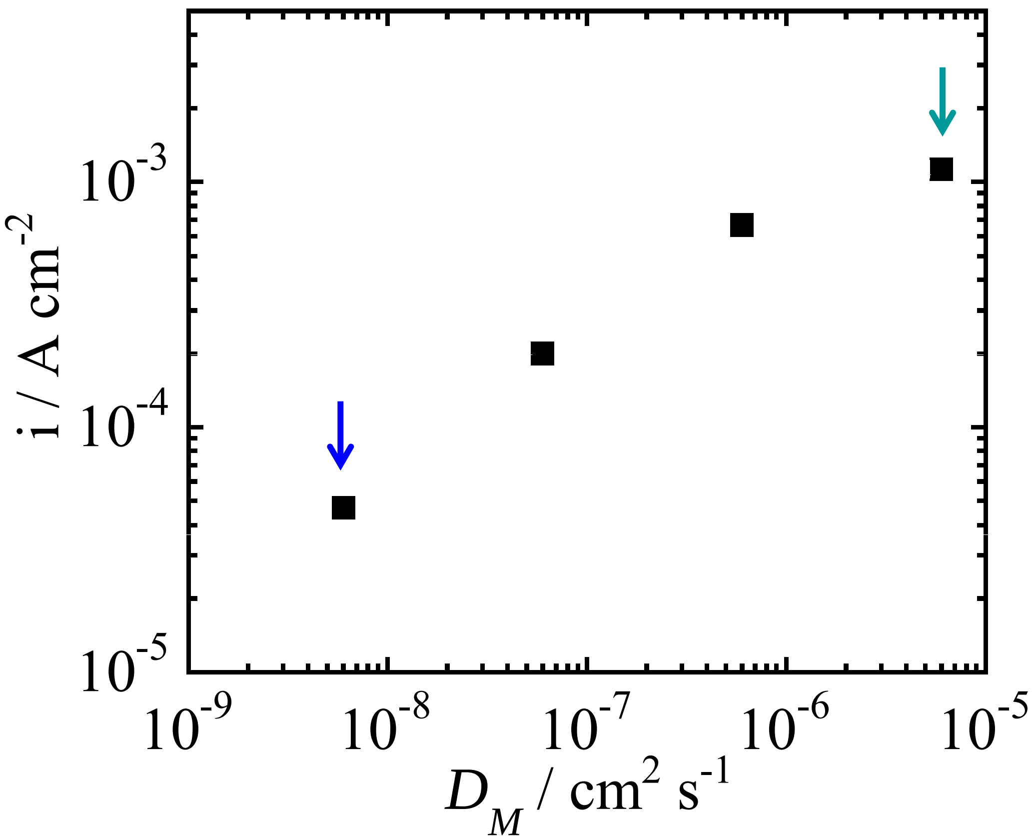

(l=50 μm)

- $D_M = 6 \times 10^{-8}$ cm^2/s : Diffusion limited (Standard redox polymer)
- $D_M = 6 \times 10^{-6}$ cm^2/s
  - Increase in i with D_M : saturated

Electrode with thick redox polymer films (l: 10^1 μm) requires high D_M

Effect of Diffusion (Electron) in Redox Polymer

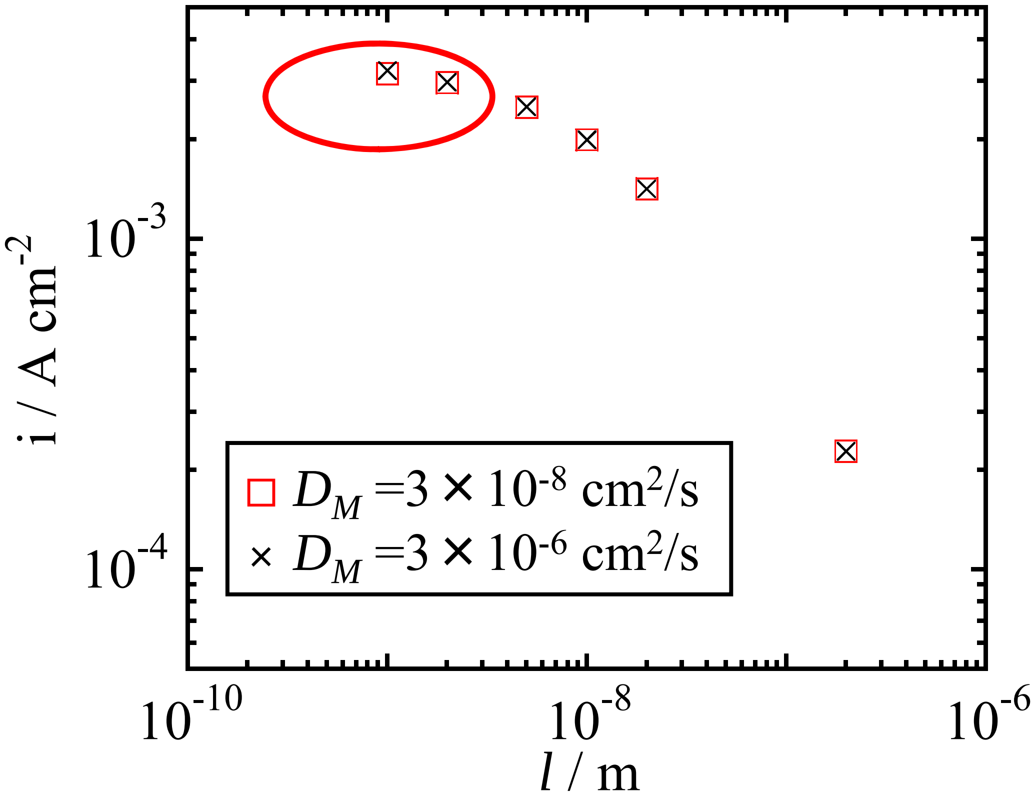

- i: Independent of D_M

< Time constant >

$$\tau(\text{Reaction}) = \frac{1}{k_{cat}} = 10^{-2} - 10^{-3}\ \text{s}$$

$$\tau(\text{Diffusion}) = \frac{l^2}{D_M} = 10^{-6} - 10^{-4}\ \text{s}$$

(D_M: 10^{-8} cm^2/s, l: 10^0-10^1 nm)

In the electrode with thin redox polymer: This study

Rate-limiting factor: Not Diffusion of electron = Reaction

-High current density can be obtained even with low D_M

T. Tamaki et al., *Fuel Cells*, accepted

Effect of Surface Coverage of Enzyme (Q_{ET})

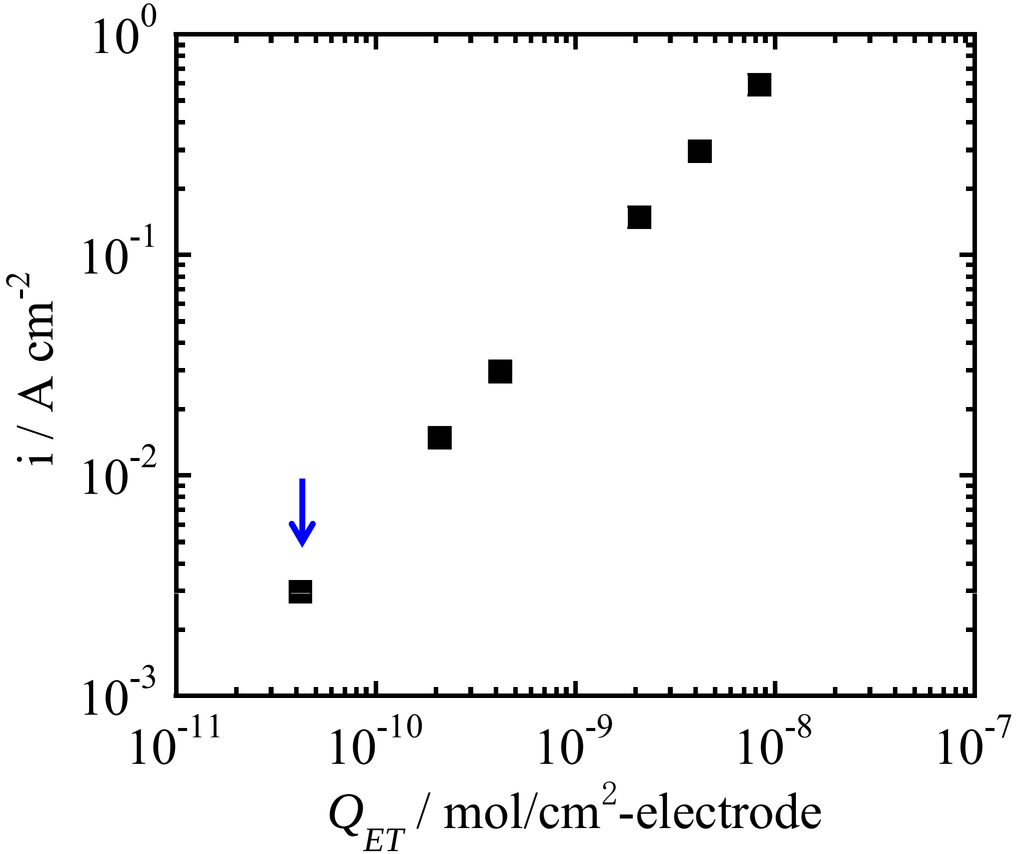

$$v_{Enz} = \frac{k_{cat} C_{Enz}}{1 + Ks / C_S + K_M / C_{MO}}$$

$$C_{Enz} = \frac{Q_{ET}}{A \times l}$$

With the increase in Q_{ET}

i increased

~ comparable to direct methanol fuel cell

Q_{ET} (This study): 4.2×10^{-11} mol/cm^2

Only one order higher than densely packed monolayer

(k_{med}, E^0_{med}: VFc, l = 2 nm, $D_M = 3 \times 10^{-8}$ cm^2/s)

Considering A_{rp} (Real surface area per projected area)= 2300, Q_{ET} might be improved

T. Tamaki et al., *Fuel Cells*, accepted

Summary

Biosystems: complex and dynamic

e.g. ion channels

and energy metabolism

New artificial device

Ion gating membrane and biofuel cell

<Powerful tool>

Combination of Material Fabrication and Mathematical Modeling